UTRECHT UNIVERSITY

BACHELOR THESIS

A comparison between low and high temperature superconductors

DECEMBER 19, 2012

Author:
Stella BOESCHOTEN

Supervisor:
Prof. dr. C. DE MORAIS SMITH
Institute for Theoretical Physics
Utrecht University

Universiteit Utrecht

Introduction

In 1911, the first superconducting material was discovered by Kamerlingh Onnes. In the years after his discovery, many other superconducting materials were found. These materials only became superconducting below a certain critical temperature T_c, which was very low, in the order of 15 K. The mechanism behind these so-called low-T_c superconductors is very well explained by the theory of Bardeen, Cooper and Schrieffer (BCS theory). However, because of the low critical temperature, their discovery was nice, but not really useful for practical applications.
In 1986, materials were discovered that became superconducting at higher temperatures, in the order of $100 - 150$ K. This lead to great excitement among physicists. However, 26 years later it is still unclear how these materials become superconducting and how their many strange properties should be explained. There are over 100.000 papers written on the subject, but there is still no satisfying theory for these high-T_c superconductors. Nevertheless, their discovery has given us hope that one day, we will be able to find materials that become superconducting around room-temperature. To find out how we should do this, we first need to fully understand the mechanism behind high-T_c superconductors. In this thesis, I will try to make clear at what point in the history of superconductivity we are, what we already know and especially what we do not know and what we hope the future will teach us.

This thesis consists of two parts. In the first part, which consists of the first two chapters, I will explain and derive the BCS theory, which is used to describe low-T_c superconductors. To do this, I need the principle of second quantization, which will be explained in chapter 1.
The second part of my thesis will be covered in chapter 3. Here, I will discuss the doping versus T phase diagram of high-T_c superconductors and the different phases that arise upon varying these paramters. The strangest of all phases is perhaps the pseudogap phase. I will try to give an overview of the different theories proposed to explain this phase.
Finally, I will make a connection between the two different parts of my thesis. I will do this based on a paper written by the group of Yazdani, in which a parallel is being made between low-T_c and high-T_c superconductors.

Acknowledgements

This thesis would not have been possible without the help of my supervisor Cristiane. She has guided me throughout the entire process of writing and spent many hours explaining the theories to me that were necessary to be able to understand what I was doing. Furthermore, she was very kind and I felt that her door always stood open for me. She even invited me into her home to celebrate Sinterklaas with her research group. I very much liked to get to know them and be able to talk about my thesis to people who knew what I was talking about. I want to thank Cristiane very much for working with me. I feel like I have learned a lot, I enjoyed it and I am very pleased with the result.

In addition, I would like to thank my parents for always being there for me and giving me the motivation to get the best out of myself. Furthermore, I want to thank my friends for providing me with the necessary distractions from my study, after which I could start working again on full power.

Contents

Chapter 1

Second quantization

Quantization in general is the process of going from a classical to a quantum theory. For example, canonical (or *first*) quantization transforms classical mechanics into quantum mechanics. In first quantization, particles are treated as quantum wave functions, while the fields are still treated classically.
However, when treating many-particle systems it is necessary to quantize the fields as well. The classical fields are replaced by the quantum-mechanical creation and destruction operators. Also, instead of using the single-particle states as a basis, a basis describing the number of particles occupying each state in a complete set of single-particle states is used. This procedure is called *second* quantization [1].
An example of second quantization can be found in the interaction between electrons. An electron interacts with a phonon, the phonon travels to another electron and causes an indirect interaction between the two electrons. Thus, this interaction between the electrons is quantized (because the number of phonons is discrete).

1.1 Occupation-number representation

For the mathematical derivations in this section, I have used refs. [2], [3].
Let $\{|\nu_1\rangle, |\nu_2\rangle, ...\}$ denote an ordered and complete single-particle basis of the N-particle Hilbert space. Actually, it is only important how many particles there are in each state $|\nu_i\rangle$, thus there must be a simpler way of representing the space, namely by just listing how many particles are present in each state. The new basis consists of elements of the form $|n_{\nu_1}, n_{\nu_2}, ...\rangle$ with the constraint that $\sum_i n_{\nu_i} = N$, where n_{ν_i} denotes the amount of particles in state ν_i. Furthermore, the basis elements are properly symmetrized or anti-symmetrized when dealing with respectively bosons or fermions. Thus we have N-particle basis states instead of the one-particle basis states from first quantization. This method is called occupation-number representation.
It now seems natural to define occupation-number operators $\hat{n}_{\nu_i}$,

$$\hat{n}_{\nu_i}|n_{\nu_i}\rangle = n_{\nu_i}|n_{\nu_i}\rangle. \tag{1.1}$$

For bosons, $n_{\nu_i} \in \mathbb{N}_{\geq 0}$, while for fermions $n_{\nu_i} \in \{0,1\}$ because of the Fermi exclusion principle.
The occupation number basis spans a space, namely the so-called Fock space $\mathcal{F}$. It is defined as $\mathcal{F} = \mathcal{F}_0 \oplus \mathcal{F}_1 \oplus \mathcal{F}_2 \oplus +...$ where $\mathcal{F}_N = span\{|n_{\nu_1}, n_{\nu_2}, ...\rangle : \sum_i n_{\nu_i} = N\}$.

Now that we have a space where the number of particles is not fixed, it makes sense to introduce a creation operator, that raises the occupation number of a state by one, and a destruction operator, that lowers the occupation number of a state by one. Because of normalization and the different properties of fermions and bosons, it turns out that these operators work as follows. For a more convenient notation, we changed the subscripts from ν_i to λ.
For bosons,

$$a_\lambda^\dagger|...,n_\lambda,...\rangle = \sqrt{n_\lambda+1}|...,n_\lambda+1,...\rangle,$$

$$a_\lambda|...,n_\lambda,...\rangle = \sqrt{n_\lambda}|...,n_\lambda-1,...\rangle,$$

and for fermions,

$$a_\lambda^\dagger|...,0,...\rangle = |...,1,...\rangle, \quad a_\lambda^\dagger|...,1,...\rangle = 0,$$

$$a_\lambda|...,1,...\rangle = |...,0,...\rangle, \quad a_\lambda|...,0,...\rangle = 0.$$

It can be shown that the creation and destruction operator satisfy certain relations. For bosons, they satisfy the commutation relations,

$$[a_\lambda, a_{\lambda'}^\dagger] = \delta_{\lambda\lambda'},$$

$$[a_\lambda, a_{\lambda'}] = [a_\lambda^\dagger, a_{\lambda'}^\dagger] = 0.$$

For fermions, they satisfy anti-commutation relations,

$$\{a_\lambda, a_{\lambda'}^\dagger\} = \delta_{\lambda\lambda'},$$

$$\{a_\lambda, a_{\lambda'}\} = \{a_\lambda^\dagger, a_{\lambda'}^\dagger\} = 0,$$

due to the antisymmetric properties of fermions. All these relations are easy to show using how $a_{\lambda'}^\dagger$ and $a_{\lambda'}$ work on a state.
It is now clear that any state can be written using creation operators on the vacuum state $|0\rangle = |0,...,0,...,0\rangle$,

$$|n_1,n_2,...\rangle = \prod_\lambda \frac{(a_\lambda^\dagger)^{n_\lambda}}{\sqrt{n_\lambda!}}|0\rangle. \tag{1.2}$$

Furthermore, it is easy to see that the number operator defined in (1.1) can also be written in terms of the creation and destruction operator, namely $\hat{n}_\lambda = a_\lambda^\dagger a_\lambda$. In general, every operator can be written as a linear combination of products of creation and destruction operators, weighed by the matrix elements of the operator calculated in first quantization. The general form for one- and two-particle operators in second quantization is

$$T_{tot} = \sum_{i,j} T_{ij} a_i^\dagger a_j, \tag{1.3}$$

$$V_{tot} = \frac{1}{2}\sum_{ijlm} V_{lmij} a_j^\dagger a_m^\dagger a_l a_i. \tag{1.4}$$

These expressions are derived in Appendix A. They hold for both fermions and bosons and for any number of particles. By using the (anti)commutation rules of a and $a^\dagger$ the symmetry of the particles is taken care of.
It is very important to put all creation operators to the left and the destruction operators to the right. This importance can be clearly illustrated with an example.
Consider a state with just one boson in state α: $a_\alpha^\dagger|0\rangle$. Then V_{tot} should always be zero because there cannot be particle-particle interaction with only one particle in the system. However, if we interchange $a_m^\dagger$ and a_l and consider $l=\alpha$ and $i=k$ then V_{tot} has a term of the form $\frac{1}{2}\sum_{mj} V_{\alpha mmj} a_j^\dagger a_m a_m^\dagger a_\alpha a_\alpha^\dagger|0\rangle = \frac{1}{2}\sum_{mj} V_{\alpha mmj} a_j^\dagger|0\rangle \neq 0$. We conclude that this term must be the particle interacting with itself. This is not particle-particle interaction, therefore we do not want this to be a part of V_{tot}. If the correct expression is used, we see $\frac{1}{2}\sum_{ijlm} V_{lmij} a_j^\dagger a_m^\dagger a_l a_i a_\alpha^\dagger|0\rangle = 0$ always holds, because there are two particles destructed after each other while there is only one in the system. Therefore this expression gives the desired result.

1.2 From first to second quantization

For this section, the refs. [1], [3], [4] have been used.
To introduce the concept of creation and destruction operators for particles, we first consider indestructible point-like bosons. Consider the Lagrangian density

$$L = i\hbar\psi^\dagger\dot{\psi} - \frac{\hbar^2}{2m}\nabla\psi^\dagger\cdot\nabla\psi - U(\mathbf{r},t)\psi^\dagger\psi. \tag{1.5}$$

The wave function ψ contains a real and imaginary part. It is possible to treat these parts as different variables. However, we will do something else namely treat ψ and $\psi^\dagger$ as different variables. Then we obtain the following,

$$\frac{\partial L}{\partial \psi} = -U(\mathbf{r},t)\psi^\dagger,$$

$$\frac{\partial L}{\partial \psi_x} = -\frac{\hbar^2}{2m}\psi_x^\dagger,$$

$$\frac{\partial L}{\partial \dot{\psi}} = i\hbar\psi^\dagger,$$

where ψ_x denotes $\nabla\psi$. Plugging the above equations into the generalized Lagrange equation yields

$$\frac{\partial L}{\partial \psi} - \nabla\frac{\partial L}{\partial \psi_x} - \frac{\partial}{\partial t}\frac{\partial L}{\partial \dot{\psi}} = -U(\mathbf{r},t)\psi^\dagger + \frac{\hbar^2}{2m}\nabla^2\psi^\dagger - i\hbar\dot{\psi}^\dagger = 0.$$

This is exactly the Hermitian conjugate of the Schrödinger equation for a particle in a potential $U(\mathbf{r})$,

$$i\hbar\dot{\psi}(\mathbf{r}) = H\psi(\mathbf{r}) = \left[-\frac{\hbar^2\nabla^2}{2m} + U(\mathbf{r})\right]\psi(\mathbf{r}).$$

The conjugate momentum is given by

$$\pi = \frac{\partial L}{\partial \dot{\psi}} = i\hbar\psi^\dagger(\mathbf{r}). \tag{1.6}$$

Now the Hamiltonian density can be obtained,

$$\mathcal{H} = \frac{\hbar^2}{2m}\nabla\psi^\dagger \cdot \nabla\psi + U(\mathbf{r},t)\psi^\dagger\psi, \tag{1.7}$$

by using $\mathcal{H} = \pi\dot{\psi} - L$. To obtain the Hamiltonian, we integrate over all volume using partial integration (the boundary term vanishes),

$$H = \int \mathrm{d}^3 r\, \mathcal{H} = \frac{\hbar^2}{2m}\left(0 - \int \mathrm{d}^3 r\, \psi^\dagger \nabla^2 \psi\right) + \int \mathrm{d}^3 r\, U\psi^\dagger\psi = \int \mathrm{d}^3 r\, \psi^\dagger \left(-\frac{\hbar^2}{2m}\nabla^2 + U\right)\psi = \int \mathrm{d}^3 r\, \psi^\dagger H_0 \psi. \tag{1.8}$$

In the equation above, H_0 denotes the one-particle Hamiltonian.
As usual, $[\psi(\mathbf{r},t), \pi(\mathbf{r}',t)] = i\hbar\delta(\mathbf{r}-\mathbf{r}')$, or using equation (1.6):

$$\left[\psi(\mathbf{r},t), \psi^\dagger(\mathbf{r}',t)\right] = \delta(\mathbf{r}-\mathbf{r}'). \tag{1.9}$$

A commutation relation like the one above is the fundamental basis of second quantization. It is actually a postulate, although the reasoning above makes intuitively clear why this is a good choice.
Let the one-particle Hamiltonian have the following eigenvalues and eigenstates,

$$H_0\phi_\lambda = \varepsilon_\lambda \phi_\lambda.$$

These eigenfunctions form a basis, hence it is possible to expand ψ and $\psi^\dagger$ in terms of this set,

$$\psi(\mathbf{r}) = \sum_\lambda a_\lambda(t)\phi_\lambda(\mathbf{r}), \tag{1.10}$$

$$\psi^\dagger(\mathbf{r}) = \sum_\lambda a_\lambda^\dagger(t)\phi_\lambda^*(\mathbf{r}). \tag{1.11}$$

Equation (1.9) is satisfied if the operators a and $a^\dagger$ satisfy the exact same commutation relations stated in Section 1.1. Here, a and $a^\dagger$ turn out to be respectively the destruction and creation operators considered in the previous section. Now, let us substitute equations (1.10) and (1.11) in (1.8). This yields the following:

$$\begin{aligned} H &= \int \mathrm{d}^3 r \sum_{\lambda,\lambda'} a_\lambda^\dagger(t)\phi_\lambda^*(\mathbf{r})\, H_0\, a_{\lambda'}(t)\phi_{\lambda'}(\mathbf{r}) = \sum_{\lambda,\lambda'} a_\lambda^\dagger a_{\lambda'} \int \mathrm{d}^3 r\, \phi_\lambda^*(\mathbf{r})\, H_0\, \phi_\lambda(\mathbf{r}) \\ &= \sum_{\lambda,\lambda'} a_\lambda^\dagger a_{\lambda'} \int \mathrm{d}^3 r\, \phi_\lambda^*(\mathbf{r})\, \varepsilon_{\lambda'}\, \phi_{\lambda'}(\mathbf{r}) = \sum_{\lambda,\lambda'} a_\lambda^\dagger a_{\lambda'} \varepsilon_{\lambda'} \int \mathrm{d}^3 r\, \phi_\lambda^*(\mathbf{r})\phi_{\lambda'}(\mathbf{r}) \\ &= \sum_{\lambda,\lambda'} a_\lambda^\dagger a_{\lambda'} \varepsilon_{\lambda'}\, \delta_{\lambda\lambda'} \\ &= \sum_\lambda \varepsilon_\lambda a_\lambda^\dagger a_\lambda. \end{aligned} \tag{1.12}$$

Hence, the Hamiltonian can be written in a simple way by using the creation and destruction operators. It consists of a set of harmonic oscillators, one for each state λ. Note that $a_\lambda^\dagger a_\lambda$ is exactly the number operator defined in Section 1.1. The Hamiltonian can always be written using these operators. In general, $H = H_0 + H_{int}$, where H_0 denotes the sum of one-particle terms and H_{int} the two-body interaction. Then, the second quantized form of H is given by

$$H = \int d\mathbf{r}\ \psi^\dagger(\mathbf{r}) H_0(\mathbf{r}) \psi(\mathbf{r}) + \int d\mathbf{r} d\mathbf{r}'\ \psi^\dagger(\mathbf{r}) \psi^\dagger(\mathbf{r}') H_{int} \psi(\mathbf{r}') \psi(\mathbf{r}). \tag{1.13}$$

Chapter 2

BCS theory

BCS theory, or Bardeen, Cooper and Schrieffer theory, is a theory which describes superconductivity in a microscopic way. Before this theory was established, there were only theories that used a macroscopic approach. In the first section of this chapter, these theories will be briefly treated, after which the BCS theory will be worked out in detail in the second section.

2.1 Historic background

For this entire section I have used ref. [5].
The history of superconductivity starts with the experiments on liquid helium of Kamerlingh Onnes in 1908. In 1911, he discovered that the resistance of mercury disappeared when he lowered the temperature below $4.19\ K$. He decided to call this new state "superconductivity". Furthermore, he found that the superconductivity disappeared when applying a certain critical magnetic field or above a certain critical current.
In 1933, Meissner and Ochsenfield discovered that a superconductor is an ideal diamagnetic, meaning that the magnetic induction $\mathbf{B}$ vanishes inside the superconductor. This effect is called the Meissner effect.
In the last century, several physicists tried to find explanations for the phenomenon of superconductivity. First, explanations were found using macroscopic theories. A thermodynamical theory using the concept of a non-measurable "order paramater" was found by Landau in 1937 and in 1935 an electrodynamical theory was established by the brothers Fritz and Heinz London. Their findings will be described in the following subsection.

2.1.1 London theory

As mentioned above, the Meissner effect states that for temperatures below the critical temperature T_c we have that $\mathbf{B} = 0$ inside the superconductor. This indicates that a magnetic field applied to a superconducting material in the normal phase is expelled to outside the material when the temperature is lowered below T_c. The Meissner effect only occurs for sufficiently low magnetic fields. Above a certain critical magnetic field H_c, the material leaves the superconducting state again.

The Londons described this effect quantitatively with their so-called London equation,

$$\nabla^2 \mathbf{B} - \frac{1}{\lambda_L^2}\mathbf{B} = 0, \qquad \lambda_L^2 = \frac{mc^2}{4\pi n_s e^2}$$

where λ_L is called the London penetration depth. To derive this equation, they primarily used electrodynamical properties of superconductors. In fact, they postulated that the left-hand side of their equation equals zero, while they only derived that it should be constant with time.
Besides the London penetration depth, there is also another characteristic length for superconductivity, namely the coherence length ξ. In microscopic theory, it describes the domain where the velocity of two electrons is correlated. Therefore, it represents the characteristic length of spatial fluctuations in a superconductor.
Using these two length scales, we can distinguish between type I and type II superconductors. For type I, we have $\lambda_L \ll \xi$ and for type II $\lambda_L \gg \xi$. The difference between these two types is the transition from the superconducting to the normal phase under application of a magnetic field. For type I, the superconducting phase is abruptly destroyed when the magnetic field exceeds H_c via a first-order phase transition. For type II, there are two critical fields H_{c1} and H_{c2} and the phase transition is of second order. The Meissner effect is total only for $H < H_{c1}$. For $H > H_{c2}$ we are in the normal phase again. However, for $H_{c1} < H < H_{c2}$ there is an intermediate phase called the vortex phase or Shubnikov phase. In this vortex phase, the flux of the magnetic field penetrates the material as a lattice of flux tubes. Each flux tube (or vortex) carries one flux quantum $\Phi_0 = hc/2e$. When increasing the magnetic field, the number of vortices increases.
Superconductors also have thermodynamical properties. In the absence of a magnetic field, the phase transition between the normal and superconducting state is of second order, meaning that there is a discontinuity in the specific heat. Furthermore, the superconducting phase represents a thermodynamical system in equilibrium with lower entropy than the normal phase.
London theory does not provide a complete macroscopic description of superconductivity. For example, only samples that are completely superconducting or completely normal can be described.

2.1.2 Ginzburg-Landau theory

It wasn't until 1950 that the most complete phenomenological theory was established by Ginzburg and Landau. They used the order parameter introduced by Landau in 1937.
Landau noticed that the mean field behaviour of the system in the neighbourhood of the phase transition is completely determined by the expansion of the free energy in terms of this order parameter. Well below T_c this expansion is no longer valid.
They also established the Ginzburg-Landau equations by minimizing the Gibbs potential. This gives

$$\frac{1}{2m^*}\left(\frac{\hbar}{i}\nabla - \frac{e^*}{c}\mathbf{A}\right)^2 \psi + \alpha\psi + \beta|\psi|^2\psi = 0,$$

$$\frac{c}{4\pi}\nabla \times \mathbf{B} = \frac{e^*\hbar}{2m^* i}(\psi^*\nabla\psi - \psi\nabla\psi^*) - \frac{e^{*2}}{m^* c}|\psi|^2\mathbf{A},$$

where ψ is the order parameter and α and β are expansion coefficients of the free energy. There is no general solution to these equations.

Similar to London theory, there are also two important length scales in Ginzburg-Landau theory, namely the Ginzburg-Landau coherence length,

$$\xi^2(T) := \frac{\hbar^2}{2m^*|\alpha|},$$

and the penetration depth,

$$\lambda^2 := \frac{m^* c^2}{4\pi e^{*2} n_s^*}.$$

There is also a third parameter, namely the Ginzburg parameter, given by $\kappa := \frac{\lambda}{\xi}$.
Using Ginzburg-Landau theory, the theory of type I and type II superconductors mentioned in Subsection 2.1.1 can be further developed. We look at samples consisting of superconducting and normal parts. We assume that there is a separation surface between these parts. To understand the behaviour of a superconductor as a function of ξ and λ, the energy σ_{ns} associated to this separation surface is studied.
Furthermore, by analyzing three different regimes, namely $\kappa \gg 1$, $\kappa \ll 1$ and $\kappa = \kappa_c$ we finally arrive at the Abrikosov classification of superconductors:

Type I: $\kappa < \frac{1}{\sqrt{2}}, \qquad \sigma_{ns} > 0$

Type II: $\kappa > \frac{1}{\sqrt{2}}, \qquad \sigma_{ns} < 0$

London already put forward the idea of flux quantization, but in the framework of Ginzburg-Landau theory it follows in a more natural way. Based on this theory, Abrikosov predicted in 1957 that a vortex lattice should appear in the superconducting material in the presence of a magnetic field.
After all this, there was still no theory that described superconductivity in a microscopic way. There were a few important experimental observations that led to the formulation of such a theory. First, the observation of an energy gap in the electronic spectrum and second, the discovery of the isotope effect (which means that the critical temperature at which superconductivity occurs depends on the mass of the atom). Because of the isotope effect, Frölich proposed in 1950 that electron-phonon interactions are responsible for superconductivity. In 1957, Bardeen, Cooper and Schrieffer used this proposal to establish their BCS theory, which is described in the next section.

2.2 BCS theory

In this section I have followed the derivation in ref. [6] and worked it out further.
John Bardeen, Leon Neil Cooper and John Robert Schrieffer proposed their theory in 1957. As mentioned at the beginning of this chapter, it is the first microscopic theory of superconductivity. An N-electron system is studied, which is a complicated problem in quantum mechanics. There are some correspondences to Bose-Einstein Condensation, but now fermions are treated, therefore we have to deal with the Fermi exclusion principle. In order to realize condensation

in our system, it is necessary that the electrons form so-called Cooper pairs. Then the state becomes boson-like. The electron-electron interaction (induced by phonons) causes an attractive potential. This potential is too weak to actually bind two electrons. Instead we get a particular collective state with N electrons (and not a more condensed state with $N/2$ pairs). In the presence of this attraction a new ground state arises, with a lower energy. As we shall see, there is an energy gap between this ground state and the first excited states. In what follows we shall determine this energy gap.
Our starting point is the following Hamiltonian,

$$H = -\frac{\hbar^2}{2m}\sum_{j=1}^{N}\nabla_j^2 + \frac{1}{2}\sum_{j\neq i}^{N} V(\vec{r}_i - \vec{r}_j),$$

where we consider V to be a two-body potential independent of spin. Now we need to rewrite this Hamiltonian into its second quantized form (that is, in terms of creation and destruction operators).
To do this, we use equations (A.1) and (A.5) from appendix A. Then, our Hamiltonian becomes

$$\begin{aligned} H &= T + V_2 \\ &= \sum_{\mathbf{k},\sigma}\frac{|\mathbf{k}|^2}{2m}a^\dagger_{\mathbf{k}\sigma}a_{\mathbf{k}\sigma} + \frac{1}{2L^3}\sum_{\substack{\mathbf{k},\mathbf{k}',\mathbf{q}\\ \sigma,\sigma'}}\widetilde{V}_2(\mathbf{q})a^\dagger_{\mathbf{k}+\mathbf{q}\sigma}a^\dagger_{\mathbf{k}'-\mathbf{q}\sigma'}a_{\mathbf{k}'\sigma'}a_{\mathbf{k}\sigma} \\ &= \sum_{k,\sigma}\varepsilon_k a^\dagger_{\mathbf{k}\sigma}a_{\mathbf{k}\sigma} + \frac{1}{2L^3}\sum_{\sigma_1,\sigma_2}\sum_{k,k',q}\widetilde{V}_2(\mathbf{q})a^\dagger_{\mathbf{k}+\mathbf{q},\sigma_1}a^\dagger_{\mathbf{k}'-\mathbf{q},\sigma_2}a_{\mathbf{k}'\sigma_2}a_{\mathbf{k}\sigma_1}, \end{aligned} \tag{2.1}$$

where $\varepsilon_k = \frac{\hbar^2k^2}{2m}$ and

$$\widetilde{V}_2(\mathbf{q}) = \int d^3\tilde{r}\, e^{-i\mathbf{q}\cdot\tilde{\mathbf{r}}}V_2(\tilde{\mathbf{r}}).$$

Now it is time to introduce the so-called "BCS-choice", namely: single-particle states are arranged in pairs $(\vec{k},\uparrow)$ and $(-\vec{k},\downarrow)$, which are simultaneously occupied or not occupied. The total spin and momentum are zero. These pairs are called Cooper pairs, because they were suggested by Cooper in 1956.
The attraction between electrons is caused by moving ions. It is legitimate to restricts its action to $-\hbar\omega_D \leq \xi_k \leq \hbar\omega_D$. Here, ω_D is the maximal frequency of a phonon (the Debye frequency), hence $\hbar\omega_D$ is the maximal energy of a phonon. We take as an assumption that the potential has the following form:

$$V_2(q) = \begin{cases} -V & \text{for} |\xi_k| \leq \hbar\omega_D \\ 0 & \text{otherwise} \end{cases}$$

Using these assumptions, we can rewrite our Hamiltonian (using $N = \sum_{\mathbf{k},\sigma}a^\dagger_{\mathbf{k}\sigma}a_{\mathbf{k}\sigma}$ and defining $\xi_k := \varepsilon_k - \mu$),

$$\begin{aligned} H - \mu N &= \sum_{k,\sigma}\xi_k a^\dagger_{\mathbf{k}\sigma}a_{\mathbf{k}\sigma} - \frac{V}{2L^3}\sum_{\sigma_1,\sigma_2}\sum_{k,k'}a^\dagger_{\mathbf{k}\sigma_1}a^\dagger_{-\mathbf{k}\sigma_2}a_{-\mathbf{k}'\sigma_2}a_{\mathbf{k}'\sigma_1} \\ &= \sum_{k,\sigma}\xi_k a^\dagger_{\mathbf{k}\sigma}a_{\mathbf{k}\sigma} - \frac{V}{2L^3}\sum_{k,k'}\left(a^\dagger_{\mathbf{k}\uparrow}a^\dagger_{-\mathbf{k}\downarrow}a_{-\mathbf{k}'\downarrow}a_{\mathbf{k}'\uparrow} + a^\dagger_{\mathbf{k}\downarrow}a^\dagger_{-\mathbf{k}\uparrow}a_{-\mathbf{k}'\uparrow}a_{\mathbf{k}'\downarrow}\right) \\ &= \sum_{k,\sigma}\xi_k a^\dagger_{\mathbf{k}\sigma}a_{\mathbf{k}\sigma} - \frac{V}{L^3}\sum_{k,k'}a^\dagger_{\mathbf{k}\uparrow}a^\dagger_{-\mathbf{k}\downarrow}a_{-\mathbf{k}'\downarrow}a_{\mathbf{k}'\uparrow}. \end{aligned} \tag{2.2}$$

For the last step, we see that the two terms yield the same after summation, because in the second term we can let $k \to -k$ and $k' \to -k'$ and interchange the two creation operators with each other and also the two destruction operators (this is possible because they commute).
In equation (2.2), μ denotes the chemical potential. It is fixed by minimizing the free energy. In first approximation, μ equals the Fermi energy E_F. The free energy is defined as

$$\Omega = -\frac{1}{\beta}\log Z,$$

where $\beta := \frac{1}{k_B T}$ and $Z = \mathrm{Tr}\, e^{-\beta(H-\mu N)}$. Z cannot be calculated exactly. Therefore, we will use a mean field approximation. For this, we use the Bogoliubov inequality:

$$\Omega \leq \Omega_m + \langle H - H_m \rangle_m := \widetilde{\Omega}, \tag{2.3}$$

where H_m is the mean field Hamiltonian. Now we are going to work out the second part of our Hamiltonian in terms of mean fields Δ and fluctuations (denoted with a prime). Then we obtain:

$$\begin{aligned}
\sum_{k,k'} a^\dagger_{\mathbf{k}\uparrow} a^\dagger_{-\mathbf{k}\downarrow} a_{-\mathbf{k}'\downarrow} a_{\mathbf{k}'\uparrow} = & \\
&= \sum_{k,k'} \left(\langle a^\dagger_{\mathbf{k}\uparrow} a^\dagger_{-\mathbf{k}\downarrow} \rangle + a'^\dagger_{\mathbf{k}\uparrow} a'^\dagger_{-\mathbf{k}\downarrow} \right) \left(\langle a_{-\mathbf{k}'\downarrow} a_{\mathbf{k}'\uparrow} \rangle + a'_{-\mathbf{k}'\downarrow} a'_{\mathbf{k}'\uparrow} \right) \\
&\simeq \sum_{k,k'} \left(\Delta + a'^\dagger_{\mathbf{k}\uparrow} a'^\dagger_{-\mathbf{k}\downarrow} \right) \left(\Delta + a'_{-\mathbf{k}'\downarrow} a'_{\mathbf{k}'\uparrow} \right) \\
&= \sum_{k,k'} \Delta^2 + \Delta \left(a'^\dagger_{\mathbf{k}\uparrow} a'^\dagger_{-\mathbf{k}\downarrow} + a'_{-\mathbf{k}'\downarrow} a'_{\mathbf{k}'\uparrow} \right) + \left(a'^\dagger_{\mathbf{k}\uparrow} a'^\dagger_{-\mathbf{k}\downarrow} \right) \left(a'_{-\mathbf{k}'\downarrow} a'_{\mathbf{k}'\uparrow} \right) \\
&\simeq \sum_{k,k'} \Delta^2 + \Delta \left(a'^\dagger_{\mathbf{k}\uparrow} a'^\dagger_{-\mathbf{k}\downarrow} + a'_{-\mathbf{k}'\downarrow} a'_{\mathbf{k}'\uparrow} \right) \\
&= \sum_{k} -\Delta^2 + \Delta \left(a^\dagger_{\mathbf{k}\uparrow} a^\dagger_{-\mathbf{k}\downarrow} + a_{-\mathbf{k}\downarrow} a_{\mathbf{k}\uparrow} \right),
\end{aligned}$$

where in the last step we plugged back in the original operators (because fluctuations are equal to the original operators minus Δ). The term Δ^2 gives us just a shift in the total energy, thus we leave it out. Our mean field Hamiltonian becomes

$$\begin{aligned}
H_m - \mu N &= \sum_{k,\sigma} \xi_k a^\dagger_{\mathbf{k}\sigma} a_{\mathbf{k}\sigma} - \frac{V}{L^3} \sum_k \Delta \left(a^\dagger_{\mathbf{k}\uparrow} a^\dagger_{-\mathbf{k}\downarrow} + a_{-\mathbf{k}\downarrow} a_{\mathbf{k}\uparrow} \right) \\
&= \sum_{k,\sigma} \xi_k a^\dagger_{\mathbf{k}\sigma} a_{\mathbf{k}\sigma} - \Delta \sum_k \left(a^\dagger_{\mathbf{k}\uparrow} a^\dagger_{-\mathbf{k}\downarrow} + a_{-\mathbf{k}\downarrow} a_{\mathbf{k}\uparrow} \right),
\end{aligned}$$

where we used $V/L^3 = 1$. We can also rewrite the first term of the Hamiltonian as follows,

$$\sum_{k,\sigma} \xi_k a^\dagger_{\mathbf{k}\sigma} a_{\mathbf{k}\sigma} = \sum_k \xi_k a^\dagger_{\mathbf{k}\uparrow} a_{\mathbf{k}\uparrow} + \xi_k a^\dagger_{\mathbf{k}\downarrow} a_{\mathbf{k}\downarrow} = \sum_k \xi_k a^\dagger_{\mathbf{k}\uparrow} a_{\mathbf{k}\uparrow} + \xi_{-k} a^\dagger_{-\mathbf{k}\downarrow} a_{-\mathbf{k}\downarrow} = \sum_k \xi_k a^\dagger_{\mathbf{k}\uparrow} a_{\mathbf{k}\uparrow} + \xi_k \left(1 - a_{-\mathbf{k}\downarrow} a^\dagger_{-\mathbf{k}\downarrow} \right)$$

This finally gives the following mean field Hamiltonian:

$$H_m - \mu N = \sum_k \xi_k \left(a^\dagger_{\mathbf{k}\uparrow} a_{\mathbf{k}\uparrow} + 1 - a_{-\mathbf{k}\downarrow} a^\dagger_{-\mathbf{k}\downarrow} \right) - \Delta \sum_k \left(a^\dagger_{\mathbf{k}\uparrow} a^\dagger_{-\mathbf{k}\downarrow} + a_{-\mathbf{k}\downarrow} a_{\mathbf{k}\uparrow} \right). \tag{2.4}$$

It is clear that the first term of this Hamiltonian is diagonal. The second term however, is not. We want to diagonalize it and to do this, we use the Bogoliubov transformation,

$$a_{\mathbf{k}\uparrow} = \cos\theta_k \alpha_{\mathbf{k}\uparrow} + \sin\theta_k \alpha^\dagger_{-\mathbf{k}\downarrow}$$

$$a^\dagger_{-\mathbf{k}\downarrow} = -\sin\theta_k \alpha_{\mathbf{k}\uparrow} + \cos\theta_k \alpha^\dagger_{-\mathbf{k}\downarrow}$$

which is actually a rotation. Because it is a canonical transformation, it satisfies the same anti-commutation relations as $a_{\mathbf{k}\sigma}$ and $a^\dagger_{\mathbf{k}\sigma}$. Plugging these transformation into the Hamiltonian (2.4) and rewriting yields:

$$\begin{aligned}
H_m - \mu N =& \sum_k \xi_k \Big(\left(\cos^2\theta_k - \sin^2\theta_k\right) \left(\alpha^\dagger_{\mathbf{k}\uparrow}\alpha_{\mathbf{k}\uparrow} - \alpha_{-\mathbf{k}\downarrow}\alpha^\dagger_{-\mathbf{k}\downarrow}\right) + 2\sin\theta_k\cos\theta_k \left(\alpha^\dagger_{\mathbf{k}\uparrow}\alpha^\dagger_{-\mathbf{k}\downarrow} + \alpha_{\mathbf{k}\uparrow}\alpha_{-\mathbf{k}\downarrow}\right) + 1 \Big) \\
& - \Delta \Big(\left(\cos^2\theta_k - \sin^2\theta_k\right) \left(\alpha^\dagger_{\mathbf{k}\uparrow}\alpha^\dagger_{-\mathbf{k}\downarrow} + \alpha_{\mathbf{k}\uparrow}\alpha_{-\mathbf{k}\downarrow}\right) - 2\sin\theta_k\cos\theta_k \left(\alpha_{\mathbf{k}\uparrow}\alpha^\dagger_{\mathbf{k}\uparrow} - \alpha_{-\mathbf{k}\downarrow}\alpha^\dagger_{-\mathbf{k}\downarrow}\right) \Big) \\
=& \sum_k \xi_k \left(\cos 2\theta_k \left(\alpha^\dagger_{\mathbf{k}\uparrow}\alpha_{\mathbf{k}\uparrow} - \alpha_{-\mathbf{k}\downarrow}\alpha^\dagger_{-\mathbf{k}\downarrow}\right) + \sin 2\theta_k \left(\alpha^\dagger_{\mathbf{k}\uparrow}\alpha^\dagger_{-\mathbf{k}\downarrow} + \alpha_{\mathbf{k}\uparrow}\alpha_{-\mathbf{k}\downarrow}\right) + 1 \right) \\
& - \Delta \left(\cos 2\theta_k \left(\alpha^\dagger_{\mathbf{k}\uparrow}\alpha^\dagger_{-\mathbf{k}\downarrow} + \alpha_{\mathbf{k}\uparrow}\alpha_{-\mathbf{k}\downarrow}\right) - \sin 2\theta_k \left(\alpha_{\mathbf{k}\uparrow}\alpha^\dagger_{\mathbf{k}\uparrow} - \alpha_{-\mathbf{k}\downarrow}\alpha^\dagger_{-\mathbf{k}\downarrow}\right) \right) \\
=& \sum_k \left(\xi_k \cos 2\theta_k + \Delta \sin 2\theta_k\right) \left(\alpha^\dagger_{\mathbf{k}\uparrow}\alpha_{\mathbf{k}\uparrow} - \alpha_{-\mathbf{k}\downarrow}\alpha^\dagger_{-\mathbf{k}\downarrow}\right) \\
& + \xi_k + \left(\xi_k \sin 2\theta_k - \Delta\cos 2\theta_k\right) \left(\alpha^\dagger_{\mathbf{k}\uparrow}\alpha^\dagger_{-\mathbf{k}\downarrow} + \alpha_{\mathbf{k}\uparrow}\alpha_{-\mathbf{k}\downarrow}\right).
\end{aligned}$$

For this expression to be diagonal, we need $\xi_k \sin 2\theta_k - \Delta\cos 2\theta_k = 0$, thus $\tan 2\theta_k = \frac{\Delta}{\xi_k}$. Then the second term in the Hamiltonian vanishes.
Now choose $-\frac{\pi}{4} \leq \theta_k \leq \frac{\pi}{4}$ such that $\cos 2\theta_k = \frac{|\xi_k|}{\sqrt{\xi_k^2+\Delta^2}}$ and $\sin 2\theta_k = \operatorname{sgn}(\xi_k)\frac{\Delta}{\sqrt{\xi_k^2+\Delta^2}}$. Using this the Hamiltonian can be rewritten:

$$\begin{aligned}
H_m - \mu N &= \sum_k \left(\xi_k \frac{|\xi_k|}{\sqrt{\xi_k^2+\Delta^2}} + \Delta \operatorname{sgn}(\xi_k) \frac{\Delta}{\sqrt{\xi_k^2+\Delta^2}} \right) \left(\alpha^\dagger_{\mathbf{k}\uparrow}\alpha_{\mathbf{k}\uparrow} - \alpha_{-\mathbf{k}\downarrow}\alpha^\dagger_{-\mathbf{k}\downarrow}\right) + \xi_k \\
&= \sum_k \xi_k + \operatorname{sgn}(\xi_k) \frac{\xi_k^2+\Delta^2}{\sqrt{\xi_k^2+\Delta^2}} \left(\alpha^\dagger_{\mathbf{k}\uparrow}\alpha_{\mathbf{k}\uparrow} - \left(1 - \alpha^\dagger_{-\mathbf{k}\downarrow}\alpha_{-\mathbf{k}\downarrow}\right)\right) \\
&= \sum_k \xi_k + \operatorname{sgn}(\xi_k)\sqrt{\xi_k^2+\Delta^2} \left(\alpha^\dagger_{\mathbf{k}\uparrow}\alpha_{\mathbf{k}\uparrow} + \alpha^\dagger_{\mathbf{k}\downarrow}\alpha_{\mathbf{k}\downarrow} - 1\right) \\
&= \sum_k \left(\xi_k - E_k + \sum_\sigma E_k \alpha^\dagger_{\mathbf{k}\sigma}\alpha_{\mathbf{k}\sigma} \right),
\end{aligned} \tag{2.5}$$

where $E_k := \operatorname{sgn}(\xi_k)\sqrt{\xi_k^2+\Delta^2}$ is the energy spectrum and in the second step we let $-k \to k$ because $E_k = E_{-k}$. From the energy spectrum it becomes clear that the values between $-\Delta$ and Δ cannot be reached. Therefore, there is a forbidden band $E_g = 2\Delta$ in the region of the Fermi energy. This band gap suggests a phase transition in which there was a kind of condensation that looks like Bose-Einstein condensation, but because of the Pauli exclusion principle electrons alone cannot condense into the same energy level. An explanation could be that the Cooper

pairs behave like bosons.
Using the Hamiltonian from equation (2.5), we calculate the partition function Z_m:

$$\begin{aligned} Z_m &= \mathrm{Tr}\ e^{-\beta(H_m-\mu N)} \\ &= \mathrm{Tr}\ e^{-\beta\sum_{k,\sigma}\left(\frac{1}{2}(\xi_k-E_k)+E_k\alpha^\dagger_{\mathbf{k}\sigma}\alpha_{\mathbf{k}\sigma}\right)} \\ &= \mathrm{Tr}\ \prod_{k,\sigma}\left(e^{-\frac{\beta}{2}(\xi_k-E_k)}e^{-\beta E_k\alpha^\dagger_{\mathbf{k}\sigma}\alpha_{\mathbf{k}\sigma}}\right) \\ &= \prod_{k,\sigma}\left(e^{-\frac{\beta}{2}(\xi_k-E_k)}\left(1+e^{-\beta E_k}\right)\right), \end{aligned}$$

and then also the Gibbs free energy Ω_m:

$$\begin{aligned} \Omega_m &= -\frac{1}{\beta}\log Z_m \\ &= -\frac{1}{\beta}\sum_{k,\sigma}\left(-\frac{\beta}{2}(\xi_k-E_k)+\log\left(1+e^{-\beta E_k}\right)\right) \\ &= \sum_{k,\sigma}\left(\frac{1}{2}(\xi_k-E_k)-\frac{1}{\beta}\log\left(1+e^{-\beta E_k}\right)\right) \end{aligned} \tag{2.6}$$

Now, to use equation (2.3), we calculate $\langle H-H_m\rangle$ using the Hamiltonians from equations (2.4) and (2.2),

$$\langle H-H_m\rangle_m = -\frac{V}{L^3}\sum_{k,k'}\langle a^\dagger_{\mathbf{k}\uparrow}a^\dagger_{-\mathbf{k}\downarrow}a_{-\mathbf{k}'\downarrow}a_{\mathbf{k}'\uparrow}\rangle_m + \Delta\sum_k\langle a^\dagger_{\mathbf{k}\uparrow}a^\dagger_{-\mathbf{k}\downarrow}+a_{-\mathbf{k}\downarrow}a_{\mathbf{k}\uparrow}\rangle_m.$$

Now we use the Bogoliubov transformation on the second term:

$$\begin{aligned} \langle a^\dagger_{\mathbf{k}\uparrow}a^\dagger_{-\mathbf{k}\downarrow}+a_{-\mathbf{k}\downarrow}a_{\mathbf{k}\uparrow}\rangle_m &= \langle\left(\cos^2\theta_k-\sin^2\theta_k\right)\left(\alpha^\dagger_{\mathbf{k}\uparrow}\alpha^\dagger_{-\mathbf{k}\downarrow}+\alpha_{-\mathbf{k}\downarrow}\alpha_{\mathbf{k}\uparrow}\right) \\ &\qquad -2\sin\theta_k\cos\theta_k\left(\alpha^\dagger_{\mathbf{k}\uparrow}\alpha_{\mathbf{k}\uparrow}-\alpha_{-\mathbf{k}\downarrow}\alpha^\dagger_{-\mathbf{k}\downarrow}\right)\rangle_m \\ &= \langle\cos 2\theta_k\left(\alpha^\dagger_{\mathbf{k}\uparrow}\alpha^\dagger_{-\mathbf{k}\downarrow}+\alpha_{\mathbf{k}\uparrow}\alpha_{-\mathbf{k}\downarrow}\right)-\sin 2\theta_k\left(\alpha^\dagger_{\mathbf{k}\uparrow}\alpha_{\mathbf{k}\uparrow}-\alpha_{-\mathbf{k}\downarrow}\alpha^\dagger_{-\mathbf{k}\downarrow}\right)\rangle_m \\ &= -\sin 2\theta_k\langle\alpha^\dagger_{\mathbf{k}\uparrow}\alpha_{\mathbf{k}\uparrow}-\alpha_{-\mathbf{k}\downarrow}\alpha^\dagger_{-\mathbf{k}\downarrow}\rangle_m \\ &= -\sin 2\theta_k\langle -1+\alpha^\dagger_{\mathbf{k}\uparrow}\alpha_{\mathbf{k}\uparrow}+\alpha^\dagger_{\mathbf{k}\downarrow}\alpha_{\mathbf{k}\downarrow}\rangle_m \end{aligned}$$

where the first term vanished because of the diagonalization of the Hamiltonian. We want to rewrite this further. To do this, we first prove the following,

$$-\frac{1}{\beta}\frac{\partial}{\partial E_k}\log Z_m = \langle -1+\alpha^\dagger_{\mathbf{k}\uparrow}\alpha_{\mathbf{k}\uparrow}+\alpha^\dagger_{\mathbf{k}\downarrow}\alpha_{\mathbf{k}\downarrow}\rangle_m,$$

by working out the left hand side,

$$\begin{aligned}
-\frac{1}{\beta}\frac{\partial}{\partial E_{k'}}\log Z_m &= -\frac{1}{\beta}\frac{1}{Z_m}\frac{\partial Z_m}{\partial E_{k'}} = -\frac{1}{\beta}\frac{1}{Z_m}\frac{\partial}{\partial E_{k'}}\operatorname{Tr} e^{-\beta\left(\sum_k \xi_k - E_k + \sum_\sigma E_k \alpha^\dagger_{\mathbf{k}\sigma}\alpha_{\mathbf{k}\sigma}\right)} \\
&= -\frac{1}{\beta}\frac{1}{Z_m}\cdot -\beta \operatorname{Tr}\left(-1+\sum_\sigma \alpha^\dagger_{\mathbf{k}'\sigma}\alpha_{\mathbf{k}'\sigma}\right) e^{-\beta(H_m-\mu N)} \\
&= \frac{1}{Z_m}\operatorname{Tr}\left(-1+\alpha^\dagger_{\mathbf{k}'\uparrow}\alpha_{\mathbf{k}'\uparrow}+\alpha^\dagger_{\mathbf{k}'\downarrow}\alpha_{\mathbf{k}'\downarrow}\right) e^{-\beta(H_m-\mu N)} \\
&= \langle -1+\alpha^\dagger_{\mathbf{k}'\uparrow}\alpha_{\mathbf{k}'\uparrow}+\alpha^\dagger_{\mathbf{k}'\downarrow}\alpha_{\mathbf{k}'\downarrow}\rangle = \langle -1+\alpha^\dagger_{\mathbf{k}\uparrow}\alpha_{\mathbf{k}\uparrow}+\alpha^\dagger_{\mathbf{k}\downarrow}\alpha_{\mathbf{k}\downarrow}\rangle.
\end{aligned}$$

Now, we work out the left hand side again, but this time using the expression for the Gibbs free energy (2.6),

$$-\frac{1}{\beta}\frac{\partial}{\partial E_k}\log Z_m = \sum_\sigma -\frac{1}{2} - \frac{1}{\beta}\frac{-\beta e^{-\beta E_k}}{1+e^{-\beta E_k}} = \sum_\sigma -\frac{1}{2}+\frac{1}{1+e^{\beta E_k}} = -1+\frac{2}{1+e^{\beta E_k}} = -(1-2f_k),$$

where we defined $f_k := \frac{1}{1+e^{\beta E_k}}$. From this we finally obtain

$$\langle a^\dagger_{\mathbf{k}\uparrow}a^\dagger_{-\mathbf{k}\downarrow} + a_{-\mathbf{k}\downarrow}a_{\mathbf{k}\uparrow}\rangle_m = \sin 2\theta_k(1-2f_k).$$

What is left is to work out the first term of $\langle H-H_m\rangle_m$, using Wick's theorem ($\langle ABCD\rangle = \langle AB\rangle\langle CD\rangle - \langle AC\rangle\langle BD\rangle + \langle AD\rangle\langle BC\rangle$ where A, B, C, D are operators). We again plug in the Bogoliubov transformations. Doing this yields

$$\begin{aligned}
a^\dagger_{\mathbf{k}\uparrow}a^\dagger_{-\mathbf{k}\downarrow} &= \cos^2(\theta_k)\alpha^\dagger_{\mathbf{k}\uparrow}\alpha_{-\mathbf{k}\downarrow} - \sin^2(\theta_k)\alpha_{-\mathbf{k}\downarrow}\alpha_{\mathbf{k}\uparrow} - \sin(\theta_k)\cos(\theta_k)\left(\alpha^\dagger_{\mathbf{k}\uparrow}\alpha_{\mathbf{k}\uparrow} - \alpha_{-\mathbf{k}\downarrow}\alpha^\dagger_{-\mathbf{k}\downarrow}\right) \\
&= \cos^2(\theta_k)\left(\alpha^\dagger_{\mathbf{k}\uparrow}\alpha_{-\mathbf{k}\downarrow}\right) - \sin^2(\theta_k)\left(\alpha_{-\mathbf{k}\downarrow}\alpha_{\mathbf{k}\uparrow}\right) - \frac{1}{2}\sin(2\theta_k)\left(-1+\alpha^\dagger_{\mathbf{k}\uparrow}\alpha_{\mathbf{k}\uparrow}+\alpha^\dagger_{\mathbf{k}\downarrow}\alpha_{\mathbf{k}\downarrow}\right), \\
a_{-\mathbf{k}'\downarrow}a_{\mathbf{k}'\uparrow} &= \cos^2(\theta_{k'})\alpha_{-\mathbf{k}'\downarrow}\alpha_{\mathbf{k}'\uparrow} - \sin^2(\theta_{k'})\alpha^\dagger_{\mathbf{k}'\uparrow}\alpha^\dagger_{-\mathbf{k}'\downarrow} - \sin(\theta_{k'})\cos(\theta_{k'})\left(\alpha^\dagger_{\mathbf{k}'\uparrow}\alpha_{\mathbf{k}'\uparrow} - \alpha_{-\mathbf{k}'\downarrow}\alpha^\dagger_{-\mathbf{k}'\downarrow}\right) \\
&= \cos^2(\theta_{k'})\left(\alpha_{-\mathbf{k}'\downarrow}\alpha_{\mathbf{k}'\uparrow}\right) - \sin^2(\theta_{k'})\left(\alpha^\dagger_{\mathbf{k}'\uparrow}\alpha^\dagger_{-\mathbf{k}'\downarrow}\right) - \frac{1}{2}\sin(2\theta_{k'})\left(-1+\alpha^\dagger_{\mathbf{k}'\uparrow}\alpha_{\mathbf{k}'\uparrow}+\alpha^\dagger_{\mathbf{k}'\downarrow}\alpha_{\mathbf{k}'\downarrow}\right).
\end{aligned}$$

Note that we could let $-k \to k$ because in the end we are summing over all k. Then we used the anti-commutating relations. Then:

$$\begin{aligned}
\langle a^\dagger_{\mathbf{k}\uparrow}a^\dagger_{-\mathbf{k}\downarrow}a_{-\mathbf{k}'\downarrow}a_{\mathbf{k}'\uparrow}\rangle_m &= \cos^2(\theta_k)\cos^2(\theta_{k'})\langle\alpha^\dagger_{\mathbf{k}\uparrow}\alpha_{-\mathbf{k}\downarrow}\rangle_m\langle\alpha_{-\mathbf{k}'\downarrow}\alpha_{\mathbf{k}'\uparrow}\rangle_m \\
&\quad + \sin^2(\theta_k)\sin^2(\theta_{k'})\langle\alpha_{-\mathbf{k}\downarrow}\alpha_{\mathbf{k}\uparrow}\rangle_m\langle\alpha^\dagger_{\mathbf{k}'\uparrow}\alpha^\dagger_{-\mathbf{k}'\downarrow}\rangle_m \\
&\quad + \frac{1}{4}\sin(2\theta_k)\sin(2\theta_{k'})\Big(\langle\alpha^\dagger_{\mathbf{k}\uparrow}\alpha_{\mathbf{k}\uparrow}\rangle_m\langle\alpha^\dagger_{\mathbf{k}'\uparrow}\alpha_{\mathbf{k}'\uparrow}\rangle_m + \langle\alpha^\dagger_{\mathbf{k}\uparrow}\alpha_{\mathbf{k}'\uparrow}\rangle_m\langle\alpha_{\mathbf{k}\uparrow}\alpha^\dagger_{\mathbf{k}'\uparrow}\rangle_m \\
&\quad + \langle\alpha^\dagger_{\mathbf{k}\uparrow}\alpha_{\mathbf{k}\uparrow}\rangle_m\langle\alpha^\dagger_{\mathbf{k}'\downarrow}\alpha_{\mathbf{k}'\downarrow}\rangle_m - \langle\alpha^\dagger_{\mathbf{k}\uparrow}\alpha_{\mathbf{k}\uparrow}\rangle_m + \langle\alpha^\dagger_{\mathbf{k}\downarrow}\alpha_{\mathbf{k}\downarrow}\rangle_m\langle\alpha^\dagger_{\mathbf{k}'\uparrow}\alpha_{\mathbf{k}'\uparrow}\rangle_m \\
&\quad + \langle\alpha^\dagger_{\mathbf{k}\downarrow}\alpha_{\mathbf{k}\downarrow}\rangle_m\langle\alpha^\dagger_{\mathbf{k}'\downarrow}\alpha_{\mathbf{k}'\downarrow}\rangle_m + \langle\alpha^\dagger_{\mathbf{k}\downarrow}\alpha_{\mathbf{k}'\downarrow}\rangle_m\langle\alpha_{\mathbf{k}\downarrow}\alpha^\dagger_{\mathbf{k}'\downarrow}\rangle_m - \langle\alpha^\dagger_{\mathbf{k}\downarrow}\alpha_{\mathbf{k}\downarrow}\rangle_m \\
&\quad - \langle\alpha^\dagger_{\mathbf{k}'\uparrow}\alpha_{\mathbf{k}'\uparrow}\rangle_m - \langle\alpha^\dagger_{\mathbf{k}'\downarrow}\alpha_{\mathbf{k}'\downarrow}\rangle_m + 1\Big)
\end{aligned}$$

$$
\begin{aligned}
&= \cos^2(\theta_k)\cos^2(\theta_{k'})f_k f_{k'}\delta_{kk'} + \sin^2(\theta_k)\sin^2(\theta_{k'})(1-f_k)(1-f_{k'})\delta_{kk'} \\
&\quad + \frac{1}{4}\sin(2\theta_k)\sin(2\theta_{k'})(f_k f_{k'} + f_k(1-f_{k'})\delta_{kk'} + f_k f_{k'} - f_k + f_k f_{k'} \\
&\quad + f_k f_{k'} + f_k(1-f_{k'})\delta_{kk'} - f_k - f_{k'} - f_{k'} + 1) \qquad (2.7) \\
&= \cos^2(\theta_k)\cos^2(\theta_{k'})f_k f_{k'}\delta_{kk'} + \sin^2(\theta_k)\sin^2(\theta_{k'})(1-f_k)(1-f_{k'})\delta_{kk'} \\
&\quad + \frac{1}{4}\sin(2\theta_k)\sin(2\theta_{k'})\left(2f_k(1-f_{k'})\delta_{kk'} + (2f_k-1)(2f_{k'}-1)\right),
\end{aligned}
$$

where we used $\langle \alpha^\dagger_{\mathbf{k}\downarrow}\alpha_{\mathbf{k}'\downarrow}\rangle_m = \langle \alpha^\dagger_{\mathbf{k}\uparrow}\alpha_{\mathbf{k}'\uparrow}\rangle_m = f_k$. Note that all terms that have a different amount of creation and destruction operators vanish because the number of particles is conserved (it can be easily seen that $N = \sum_{k,\sigma}\alpha^\dagger_{k\sigma}\alpha_{k\sigma}$ commutes with the Hamiltonian $H_m - \mu N$). The terms where spin is not conserved also vanish. We repeatedly used Wick's theorem as stated above. The terms proportional to $\delta_{kk'}$ vanish in the thermodynamical limit thus we obtain:

$$
\langle a^\dagger_{\mathbf{k}\uparrow}a^\dagger_{-\mathbf{k}\downarrow}a_{-\mathbf{k}'\downarrow}a_{\mathbf{k}'\uparrow}\rangle_m = \frac{1}{4}\sin(2\theta_k)\sin(2\theta_{k'})(2f_k-1)(2f_{k'}-1).
$$

Plugging our results into $\langle H - H_m\rangle_m$ yields

$$
\begin{aligned}
\langle H - H_m\rangle_m &= -\frac{V}{L^3}\sum_{k,k'}\langle a^\dagger_{\mathbf{k}\uparrow}a^\dagger_{-\mathbf{k}\downarrow}a_{-\mathbf{k}'\downarrow}a_{\mathbf{k}'\uparrow}\rangle_m + \Delta\sum_k\langle a^\dagger_{\mathbf{k}\uparrow}a^\dagger_{-\mathbf{k}\downarrow} + a_{-\mathbf{k}\downarrow}a_{\mathbf{k}\uparrow}\rangle_m \\
&= -\frac{V}{L^3}\sum_{k,k'}\frac{1}{4}\sin 2\theta_k \sin 2\theta_{k'}(1-2f_k)(1-2f_{k'}) + \Delta\sum_k \sin 2\theta_k(1-2f_k) \\
&= -\frac{V}{L^3}\left(\frac{1}{2}\sum_k \sin 2\theta_k(1-2f_k)\right)^2 + \Delta\sum_k \sin 2\theta_k(1-2f_k).
\end{aligned}
$$

Furthermore, $1-2f_k = \frac{e^{\beta E_k}+1-2}{e^{\beta E_k}+1} = \frac{e^{\frac{1}{2}\beta E_k} - e^{-\frac{1}{2}\beta E_k}}{e^{\frac{1}{2}\beta E_k} + e^{-\frac{1}{2}\beta E_k}} = \tanh(\frac{1}{2}\beta E_k)$. Using this, it follows from the Bogoliubov inequality that

$$
\begin{aligned}
\widetilde{\Omega} = \Omega_m + \langle H - H_m\rangle_m &= \sum_k\left(\xi_k - E_k - \frac{2}{\beta}\log\left(1+e^{-\beta E_k}\right)\right) + \Delta\sum_k \sin 2\theta_k \tanh\left(\frac{1}{2}\beta E_k\right) \\
&\quad - \frac{V}{L^3}\left(\frac{1}{2}\sum_k \sin 2\theta_k \tanh(\frac{1}{2}\beta E_k)\right)^2 \\
&= \sum_k\left(\xi_k - E_k - \frac{2}{\beta}\log\left(1+e^{-\beta E_k}\right) + \frac{\Delta^2}{E_k}\tanh\left(\frac{1}{2}\beta E_k\right)\right) \\
&\quad - \frac{V}{L^3}\left(\frac{1}{2}\sum_k \frac{\Delta}{E_k}\tanh\left(\frac{1}{2}\beta E_k\right)\right)^2,
\end{aligned}
$$

where we used $\sin 2\theta_k = \frac{\Delta}{\mathrm{sgn}(\xi_k)\sqrt{\xi_k^2+\Delta^2}} = \frac{\Delta}{E_k}$.

To determine the gap or effective field Δ we minimize $\widetilde{\Omega}$. Note that

$$
\frac{dE_k}{d\Delta} = \mathrm{sgn}(\xi_k)\frac{2\Delta}{2\sqrt{\xi_k^2+\Delta^2}} = \frac{\Delta}{E_k}.
$$

Subsequently, define $f(\Delta) := \sum_k \frac{\tanh(\frac{1}{2}\beta E_k)}{E_k}$. Then taking the derivative yields:

$$\begin{aligned}
\frac{d\Omega}{d\Delta} &= \frac{d}{d\Delta}\sum_k \left(\xi_k - E_k - \frac{2}{\beta}\log\left(1+e^{-\beta E_k}\right)\right) + \Delta^2 f(\Delta) - \frac{V}{L^3}\left(\frac{1}{2}\Delta f(\Delta)\right)^2 \\
&= \sum_k -\frac{\Delta}{E_k}\left(1 - \frac{2e^{-\beta E_k}}{1+e^{-\beta E_k}}\right) + 2\Delta f(\Delta) + \Delta^2 f'(\Delta) - \frac{V}{2L^3}\Delta f^2(\Delta) - \frac{V}{2L^3}\Delta^2 f(\Delta) f'(\Delta) \\
&= \sum_k -\frac{\Delta}{E_k}\tanh(\frac{1}{2}\beta E_k) + 2\Delta f(\Delta) + \Delta^2 f'(\Delta) - \frac{V}{2L^3}\Delta f^2(\Delta) - \frac{V}{2L^3}\Delta^2 f(\Delta) f'(\Delta) \\
&= \Delta f(\Delta) + \Delta^2 f'(\Delta) - \frac{V}{2L^3}\Delta f^2(\Delta) - \frac{V}{2L^3}\Delta^2 f(\Delta) f'(\Delta) \\
&= \left(\Delta - \frac{V}{2L^3}\Delta f(\Delta)\right)\left(f(\Delta) + \Delta f'(\Delta)\right).
\end{aligned}$$

To minimize $\widetilde{\Omega}$ we set this to zero. The second term is always larger than zero thus the first term must be zero. The gap equation becomes

$$\Delta = \frac{V}{2L^3}\sum_k \frac{\Delta}{E_k}\tanh\left(\frac{1}{2}\beta E_k\right), \tag{2.8}$$

where we plugged back in the definition for $f(\Delta)$. One solution for this equation is obviously $\Delta = 0$. This solution corresponds to the normal metal. Other solutions of the gap equation can be found using some approximations.
Assume $\Delta \neq 0$. Then we can divide both sides of the gap equation by Δ. We transform the sum into an integral; $\frac{1}{L^3}\sum_k \to \int \frac{d^3k}{(2\pi)^3}$. This gives:

$$\begin{aligned}
2 &= V\int \frac{d^3k}{(2\pi)^3}\frac{1}{E_k}\tanh\left(\frac{1}{2}\beta E_k\right) \\
&= V\int \frac{d^3k}{(2\pi)^3}\frac{\mathrm{sgn}(\xi_k)}{\sqrt{\xi_k^2+\Delta^2}}\tanh\left(\frac{\beta}{2}\sqrt{\xi_k^2+\Delta^2}\,\mathrm{sgn}(\xi_k)\right) \\
&= V\int \frac{4\pi k^2 dk}{8\pi^3}\frac{1}{\sqrt{\xi_k^2+\Delta^2}}\tanh\left(\frac{\beta}{2}\sqrt{\xi_k^2+\Delta^2}\right) \\
&= V\frac{1}{2\pi^2}\int dk\, k^2 \frac{1}{\sqrt{\xi_k^2+\Delta^2}}\tanh\left(\frac{\beta}{2}\sqrt{\xi_k^2+\Delta^2}\right) \\
&= V\frac{1}{2\pi^2}\int d\xi \left.\frac{dk}{d\xi}\right|_{\xi=0} k^2 \frac{1}{\sqrt{\xi_k^2+\Delta^2}}\tanh\left(\frac{\beta}{2}\sqrt{\xi_k^2+\Delta^2}\right) \\
&= VN(E_F)\int_0^{\hbar\omega_D} d\xi \frac{1}{\sqrt{\xi_k^2+\Delta^2}}\tanh\left(\frac{\beta}{2}\sqrt{\xi_k^2+\Delta^2}\right),
\end{aligned}$$

where $N(E_F) = \frac{1}{2\pi^2}k^2 \left.\frac{dk}{d\xi}\right|_{\xi=0}$ is the density of states. We now have a non-linear equation for Δ. The right hand side decreases as a function of T and Δ. Consequently, Δ becomes smaller

when T increases until T_c. For $T = 0$ we have $\beta \to \infty$ thus the hyperbolic tangent goes to one. We obtain:

$$\begin{aligned}
2 &= VN(E_F) \int_0^{\hbar\omega_D} d\xi \frac{1}{\sqrt{\xi_k^2 + \Delta^2}} \\
&= \frac{VN(E_F)}{\Delta} \int_0^{\hbar\omega_D} d\xi \frac{1}{\sqrt{1 + \left(\frac{\xi}{\Delta}\right)^2}} \\
&= VN(E_F) \int_0^{\frac{\hbar\omega_D}{\Delta}} dx \frac{1}{\sqrt{1+x^2}} \\
&= VN(E_F) \sinh^{-1}\left(\frac{\hbar\omega_D}{\Delta}\right).
\end{aligned}$$

Rewriting this gives:

$$\begin{aligned}
\Delta(0) &= \frac{\hbar\omega_D}{\sinh\left(\frac{2}{VN(E_F)}\right)} \\
&= 2\hbar\omega_D \frac{1}{e^{\frac{2}{VN(E_F)}} - e^{-\frac{2}{VN(E_F)}}} \\
&\simeq 2\hbar\omega_D e^{-\frac{2}{VN(E_F)}},
\end{aligned}$$

where in the last step we assumed $VN(E_F) \ll 1$.
Now we take the limit $T \to T_c$. Then $\Delta \to 0$, thus

$$2 \simeq VN(E_F) \int_0^{\hbar\omega_D} d\xi \, \frac{1}{\xi} \tanh\left(\frac{1}{2}\beta_c \xi\right)$$

Consequently,

$$\begin{aligned}
\frac{2}{VN(E_F)} &= \int_0^{\frac{1}{2}\beta_c\hbar\omega_D} dx \, \frac{\beta_c}{2x} \frac{2}{\beta_c} \tanh x \\
&= \int_0^{\frac{1}{2}\beta_c\hbar\omega_D} dx \, \frac{\tanh x}{x} \\
&= \log x \tanh x \Big|_0^{\frac{1}{2}\beta_c\hbar\omega_D} - \int_0^{\frac{1}{2}\beta_c\hbar\omega_D} dx \, \frac{\log x}{\cosh^2 x} \\
&\simeq \log\left(\frac{1}{2}\beta_c\hbar\omega_D\right) + \log 4\frac{e^\gamma}{\pi} \\
&= \log\left(2\beta_c\hbar\omega_D \frac{e^\gamma}{\pi}\right),
\end{aligned}$$

where we assumed that $\frac{1}{2}\beta_c\hbar\omega_D$ is large thus the hyperbolic tangent is approximately equal to one. Furthermore, $e^\gamma \simeq 1.781$. From this it follows that

$$k_B T_c \simeq 2\hbar\omega_D \frac{e^\gamma}{\pi} e^{-\frac{2}{VN(E_F)}}. \tag{2.9}$$

Define $E_g = 2\Delta(0)$. Then:

$$\frac{E_g}{k_B T_c} = \frac{4\hbar\omega_D e^{-\frac{2}{VN(E_F)}}}{2\frac{e^\gamma}{\pi}\hbar\omega_D e^{-\frac{2}{VN(E_F)}}} = \frac{2\pi}{e^\gamma} \simeq 3.52790 \tag{2.10}$$

This is an universal result and it has a surprisingly good agreement with experiments. This can be seen in the following table, where E_g is obtained by measuring $H_c(0)$ and the specific heat.

Supra	$E_g/k_B T_c$	Supra	$E_g/k_B T_c$
Al	3.53	Nb	3.65
Cd	3.44	Pb	3.95
Ga	3.5	Sn	3.6
Hg	3.95	Ta	3.63
In	3.65	Tl	3.63
La	3.72	Zn	3.44

Chapter 3

High-temperature superconductors

The theory we have discussed so far gives a good description of superconductors with critical temperatures T_c up to 30 K. However, in 1986 a superconductor with $T_c \approx 35\ K$ was discovered by K.A. Müller and J.G. Bednorz, for which they were awarded with the Nobel Prize in Physics a year later. Surprisingly, they were not looking at metals, but at insulating materials (copper oxides).
These kind of superconductors are called high-T_c superconductors. Critical temperatures up to 138 K have been measured. The first high-T_c superconductors, called "cuprates" all contained copper and oxygen atoms. Later, also high-temperature superconductors containing iron or arsenic (called "pnictides") were discovered. For all these newly discovered superconductors, BCS theory did not give an appropriate description. It is still unknown how this new kind of superconductivity works.
In the first section of this chapter, I will start with a discussion of the cuprates. In the next two sections, I will discuss the different phases of the cuprates and describe the theories proposed to explain them. This chapter is mainly based on ref. [7]. Other references will be given in the text.

3.1 Cuprates

As mentioned above, cuprates contain copper and oxygen atoms, and also atoms like Ba, Tl and La. The copper and oxygen atoms form CuO_2 planes separated by layers of these other atoms. These layers are often seen as charge reservoirs, because they supply charge carriers to the CuO_2 planes. The copper and oxygen atoms are arranged in a so-called Lieb lattice, see figure 3.1 below. The blue dots denote copper atoms and the green dots oxygen atoms. However, we study the simplified lattice where the oxygen atoms are not taken into account.
All cuprates are antiferromagnetic insulators. They only become superconducting when a certain amount of dopant is added. Depending on the kind of dopant, two things can happen. The material can become hole-doped, if there are fewer electrons donated to the CuO_2 planes, or electron-doped, if there are more electrons donated to the CuO_2 planes. In both cases, a superconducting region is formed. This is why it is believed that superconductivity takes places in the CuO_2 planes.
To make this more clear, I will now give an example, namely LSCO (La_2SrCuO_4). LSCO consists of single CuO_2 planes, seperated by two LaO layers. The electron configuration of the different atoms is as follows: Cu: $[\mathrm{Ar}](3d)^{10}(4s)$; La: $[\mathrm{Xe}](5d)(6s)^2$ and O: $[\mathrm{He}](2s)^2(2p)^4$.

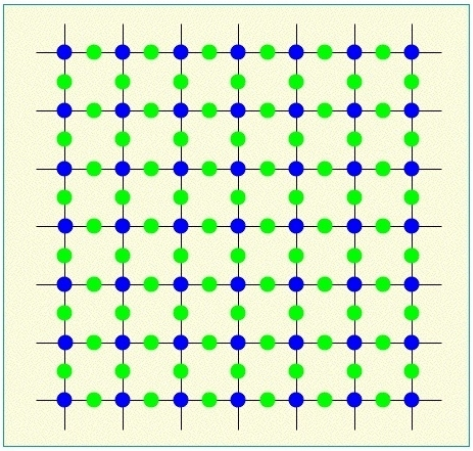

Figure 3.1: Lieb lattice

In the crystal, oxygen takes up two electrons such that it becomes [He]$(2s)^2(2p)^6$ and lanthanum loses three electrons such that is becomes [Xe]. To guarantee charge neutrality, this means that copper has a $2+$ charge, such that its electronic configuration is [Ar]$(3d)^9$. Thus, there is a hole in the d-shells of the copper atoms. These holes can have spin up or down and they arrange themselves antiferromagnetically (below the Néel temperature, because above it the material becomes paramagnetic). There is exactly one hole per copper site; this is called half-filling.
Upon doping with Sr (with electron configuration [Kr]$(5s)^2$), some of the La^{3+} are replaced by Sr^{2+}, such that we have $La_{2-x}Sr_xCuO_4$, where x denotes the amount of added dopant. In general x is very small. This means that there are fewer electrons donated to the CuO_2 planes, such that oxygen changes its configuration from O^{2-} to O^-. This results in a hole in the p-shell of oxygen. Nevertheless, in an effective description one considers a hole in the Cu lattice because we ignored the oxygen atoms. This means that we go from a square lattice with spin $\frac{1}{2}$ on every site to a square lattice where a few sites have spin zero in a background of spin $s = \frac{1}{2}$. The sites where $s = 0$ contain a spin singlet of one electron with spin up and one electron with spin down, called a Zhang-Rice singlet. They are also called holes and function as charge carriers.
When the dopant is added, the system first goes through a spin glass phase and then it exhibits a superconducting phase, which has a dome slope. When T_c is increasing, the system is called underdoped and when it is decreasing it is called overdoped. The amount of doping for which T_c is maximal is called optimally doped.
If we increase the temperature sufficiently when in the superconducting state, a phase transition to the normal state occurs. This normal state is actually not so normal, since it has many unusual properties, part of which cannot be described by Fermi liquid theory. I will discuss this further in section 3.3.
Another hole-doped cuprate is YBCO, $YBa_2Cu_3O_{7-x}$. In this material, there are CuO chains in the charge reservoir, at which oxygen atoms are added as dopant. Furthermore, YBCO has two CuO_2 planes instead of one, and also a relatively high critical temperature of approximately 92 K. This suggests that more CuO_2 layers result in a higher T_c. However, it turns out that this only holds up to three layers. Together with BiSCCO ($Bi_2Sr_2CaCu_2O_{8+x}$), LSCO and YBCO are the most studied hole-doped cuprates.
Electron-doped materials, such as $Nd_{2-x}Ce_xCuO_4$, have a more robust antiferromagnetic phase,

a smaller superconducting dome and often a lower critical temperature compared to hole-doped materials. Because of this, we will not discuss electron-doped materials any further.

3.2 The superconducting state

3.2.1 Validity of BCS

There have been many attempts to find a way to explain high-T_c superconductivity within the framework of BCS theory. For example, the spin singlets (holes) could be seen as something equivalent to the Cooper pairs. Furthermore, BCS theory describes superconductors through a retarded phonon mediated interaction between the electrons. This kind of interaction is not able to explain the high critical temperatures found in the cuprates. Namely, BCS theory incorporates the isotope effect, which is an experimentally confirmed effect saying that the critical temperature is inversely proportional to the mass of the isotope used in the superconducting material. However, in cuprates there is a negligible change in T_c when an isotope is substituted. Because of this, people started searching for a different interaction, mediated by something else than phonons. Other quasiparticles such as excitons and polarons were considered, but the most popular view was an interaction mediated by spin fluctuations.
Subsequently, for BCS theory to work we need the normal phase to be a Fermi liquid. A Fermi liquid is basically a system of strongly interacting particles, that can also be described by an equivalent system of non- or weakly interacting quasiparticles. This theory was established by Landau. It is necessary to have a Fermi liquid because we need an instability within the Fermi surface for BCS to work. However, it seems that the normal state of a cuprate is only a Fermi liquid at high dopings, but not for small and intermediate dopings at high temperatures.

3.2.2 More differences between conventional and high-T_c superconductors

Besides the differences between conventional and high-T_c superconductors mentioned above, there are some other important differences. A few of them are listed below and shortly discussed.

- The coherence length ξ of cuprates is much smaller, resulting in a lower superfluid stiffness (ξ represents the characteristic length of spatial fluctuations). Furthermore, the in-plane coherence length is larger than the coherence length orthogonal to the plane.
- Retardation effects in cuprates are very small.
- Lattice properties are less important. For example: in a conventional superconductor, application of an external pressure leads to a stiffening of the lattice and thus a lowering of T_c. In high-T_c superconductors different effects occur in different materials if an external pressure is applied.
- The symmetry of the order parameter of cuprates is $d_{x^2-y^2}$ (this is found using SQUID magnetometry), which means that the pairing wave function changes sign four times as a function of angle. The pairing wave function is roughly equal to the superconducting gap $\Delta(\mathbf{k}) = \langle a^\dagger_{\mathbf{k}\uparrow} a^\dagger_{-\mathbf{k}\downarrow} \rangle$. Therefore, $\Delta(\mathbf{k})$ vanishes for certain direction in k-space. This

results in the existence of nodal lines, i.e. quasiparticle excitations in these directions cost no energy. Actually it turns out that the system is not truly d-wave, but it is d-wave *like*. Conventional superconductors are s-wave, which means that the gap function has no nodes and is independent of momentum.

- The main component of a cuprate is a Mott insulator, and not a conducting metal. Because of this, we should perhaps treat cuprates as doped Mott insulators and not as strongly interacting metals.

3.3 The normal state

In the phase diagram of a cuprate, the Mott insulating phase is very close to the superconducting phase. This makes the normal (non-superconducting) state of a cuprate very difficult to describe. Actually, we have to distinguish between the under- and overdoped regions and the region around optimal doping. When doing this, one can differentiate several phases, that can be seen in figure 3.2 below. However, the distinction between different regions in the phase diagram is not always well-defined. Thus, some transitions should be seen merely as cross-overs. Far in the overdoped regime, the cuprate can be described as an ordinary Fermi liquid. Close to the optimally doped regime, we have the strange metal phase and in the underdoped regime we have the so-called pseudogap phase. Around zero doping, the system behaves as an insulating antiferromagnet. In the next subsections, I will briefly discuss the pseudogap phase and the strange metal phase.

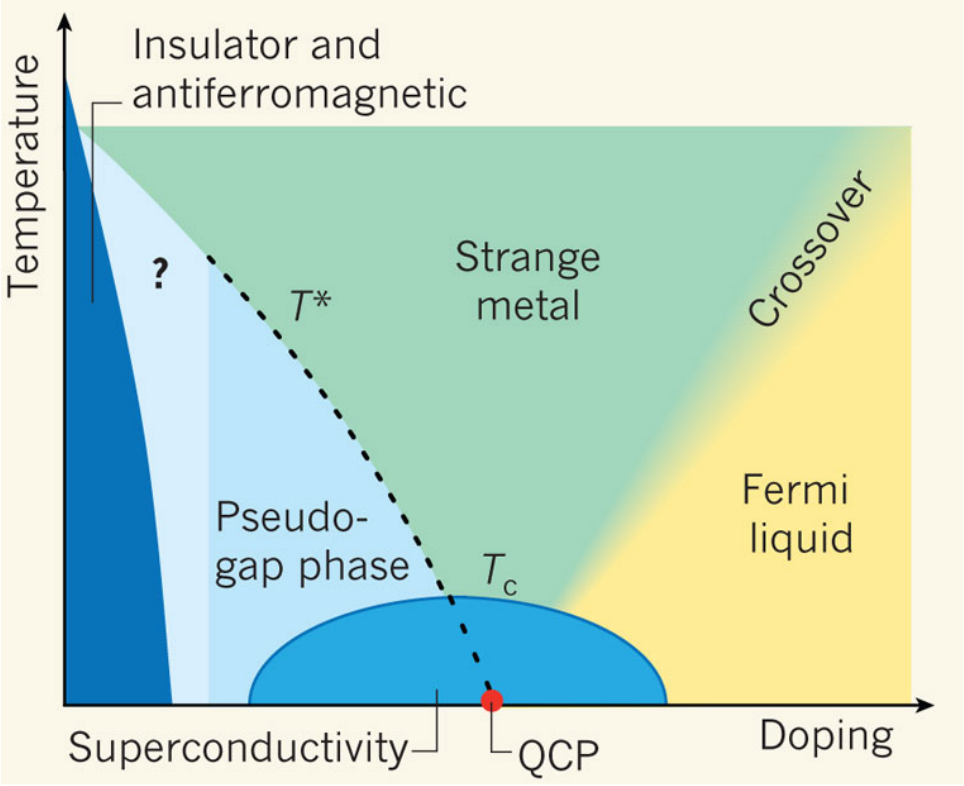

Figure 3.2: Phase diagram of the cuprates [8]

3.3.1 Strange metal

In the regime between the pseudogap phase and the Fermi liquid, we have a phase called strange metal, or also marginal Fermi liquid. In the overdoped regime at low temperatures, the system behaves as a Fermi liquid. There are only quasiparticles, resulting in an in-plane resistivity $\rho \sim T^2$. Upon raising the temperature, phonons become more important and for high T we would expect the resistance to be independent of T because it only depends on the vibration of the electrons. However, it turns out that this is not the case. Around the optimally doped regime, $\rho \sim T$. Furthermore, it turns out that the Hall coefficient in the strange metal phase is strongly temperature dependent, while we would expect it to be independent of T. All these strange properties lead to the conclusion that this phase cannot be described as a Fermi liquid. An explanation of these properties could be given by quantum criticality. Some physicists propose the existence of a quantum critical point (QCP) in the phase diagram of a cuprate, also indicated in figure 3.2. At a QCP a phase transition takes place at $T = 0$. Conventional phase transitions are driven by critical fluctuations, that are limited to a small region around the phase transition. However, when looking at quantum phase transitions, the fluctuations have a quantum mechanical nature. These fluctuations can still be felt in a wide range of temperatures above the QCP, thus quantum criticality has important effects even if $T = 0$ is never reached. In the region above a quantum critical point a universal behaviour is observed. On average, the system looks the same regardless of the length- and time scale on which it is observed. Because the current is carried by those quantum fluctuations, the linear resistivity can be explained. However, it is unclear whether the quantum critical point actually exists in this case. Because the QCP should be within the superconducting region, its appearance may be obscured and difficult to locate experimentally. However, there have been transport experiments at which a large magnetic field was applied to suppress superconductivity. These experiments suggested that a phase transition between an insulating state for $x < x_c$ and a metallic state for $x > x_c$ indeed takes place at zero temperature [9].

3.3.2 Pseudogap phase

The pseudogap phase is the region bordered by the antiferromagnetic phase on the left and the strange metal and superconducting phase on the right. This is probably the most complicated and unexplained part of the phase diagram. Lots of experiments have been done in this region, but they all suggests a different explanation for the behaviour of the system in the pseudogap phase. As the name says, in the pseudogap phase there exist certain pseudogaps. When there is a gap in the energy range, this means that there is a certain range where no states are allowed. Subsequently, the presence of a *pseudo*gap indicates that there is an energy range that contains only a small amount of states. A gap should indicate an insulating state. However, when looking at a pseudogap, it turns out that only electrons travelling in the direction of the Cu-O bonds are affected by its presence. Electrons moving in a direction 45 degrees to this bond can move freely through the crystal. In the superconducting region, there is a gap everywhere except at the nodal points (due to the d-wave nature of the cuprates). Upon raising the temperature above T_c, in momentum space these points grow into so-called Fermi arcs. When the temperature is raised even further, finally the four arcs meet and form a connected Fermi surface. Only on these arcs the spectrum is gapless, and outside the arcs the pseudogap exists. Thus, this system does not have a well-defined Fermi surface. Some experiments point out that there are actually

two pseudogaps, one at low temperatures and one at slightly higher temperatures.
So far, there is no theory that describes systems without a well-defined Fermi surface. There are several theories that try to give a description of the pseudogap phase, but none of them has been fully accepted by all physicists. In what follows I will describe two theories that are quite popular.

3.3.2.1 Competing orders

One of these theories proposes that in the pseudogap phase there are all kinds of different orders present, consisting for example of charge segregations (stripes and quantum liquid crystals) but also of hidden orders such as spontaneous diamagnetic currents. There is experimental evidence for many of those types of order, indicating that they might compete and even coexist with each other. It is still unclear whether these types of order are promoting or competing against superconductivity. I will discuss two of these orders, namely stripes and spontaneous diamagnetic current phases (staggered π-flux phase and Varma phase).

Stripes In section 3.1 we explained that upon adding dopant to a cuprate, holes appear in the lattice. The dynamics of these holes in an antiferromagnetic background were studied by Jan Zaanen and Olle Gunnarsson in 1989. In their study, they also took into account the previously ignored oxygen atoms in the CuO_2 planes. They proposed that the holes in the doped cuprate do not distribute themselves homogeneously in the antiferromagnetic background, but form lines. This proposal is based on their solution of the three-band Hubbard model close to half-filling ($s = \frac{1}{2}$ on every site) at zero temperature. The formed lines are called stripes. There are several explanations for their existence. For example, they can be explained to arise as a competition between a short-range effective attractive interaction, which makes the system split into two phases (a hole-rich phase and an antiferromagnetic phase) in order to break as few antiferromagnetic bonds as possible and the holes distributing themselves homogeneously due to long-range Coulomb repulsion. The stripes can also be explained, because they minimize the kinetic energy by making sure that the spins in the antiferromagnetic phase do not misalign. In this way, the stripes act as domain walls between different Mott insulating domains. When such a domain wall is crossed, the magnetization changes by π.
Most stripes found in doped cuprates are dynamical, i.e. they fluctuate. There are also static stripes in some of the cuprates, for example in LSCO after it is co-doped with Nd. Static stripes were also found in some non-superconductors, suggesting that they do not stimulate superconductivity and maybe even compete with it. However, if the stripes are not too static, the Yamada plot suggests that they could promote superconductivity, because it seems that T_c increases when the stripes move closer together.
The presence of dynamical stripes could now give a possible explanation for the development of superconductivity in cuprates, namely: when doping the cuprate when in the antiferromagnetic phase, holes start to appear. Upon adding more dopant, more holes appear and order themselves in dynamical stripes, partially destroying the antiferromagnetic phase. When more stripes are formed, they start filling the entire CuO_2 planes and become phase coherent. Finally, when stripes from different planes couple to each other, we have true long range superconductivity.

Spontaneous diamagnetic current phases When Affleck and Marston were solving the one-band Hubbard model in mean-field treatment, they proposed that the hopping parameter in the Hamiltonian should be complex. If this is indeed true, it means that there is a vector potential that should be taken into account. Consequently, there will be staggered currents on the copper lattice, i.e there is an alternation between a clockwise and a counter-clockwise current on neighbouring lattice sites. As a result, time reversal symmetry and lattice translational symmetry are broken (the primitive lattice site becomes twice as large). This phase is called the staggered π-flux phase.
Chandra Varma proposed a theory similar to the one described above, except that he thought that the oxygen atoms of the CuO_2 planes cannot be neglected. He proposed a phase where the currents are not flowing around a lattice site as in the π-flux phase. Instead, the current flows from copper to oxygen and again to oxygen and then back to the first copper in a little triangle. There are two such triangles per lattice site and the currents flow in different directions in each of them such that the total current per plaquette is zero. There are many different types of this so-called Varma phase, but they all have the property that each lattice site is the same. This means that the lattice translation symmetry is not broken. However, time reversal symmetry remains broken. Recent experiments have pointed out that in the pseudogap phase time reversal symmetry is indeed broken and the overall measurements were more consistent with the Varma phase than with the π-flux phase.

3.3.2.2 Non simultaneous phase coherence and pair creation

An important experimental investigation of the pseudogap phase was performed by the group of Yazdani in Princeton. In this section I will discuss their article, ref. [10].
As mentioned above, in high temperature superconductors there is a partial gap in the density of states for a range of temperatures above T_c. The main questions that Yazdani *et al.* are trying to answer are whether this gap is associated with pairing and what is determining the temperature at which pairs start to form. To answer these questions, they were the first that did spatially resolved measurements on gap formation in the cuprate BiSCCO, with doping levels in the range $0.12 - 0.22$, using STM (scanning tunnelling microscopy, see appendix B). For their experiments, they used a specially designed variable temperature ultrahigh-vacuum STM to be able to track specific areas of the sample on the atomic scale as a function of T.

First, they looked at a specific site in the most overdoped sample (OV65, where OV stands for overdoped and 65 for the critical temperature in Kelvin), with a doping level of $x = 0.22$. They measured spectra over a range of temperatures close to T_c, from which they deduced the maximal value of the local gap and the temperature T_p at which the gap is no longer measurable. Subsequently, this measurement was repeated on many other sites, resulting in spectroscopic mapping measurements over areas ~ 300 Å. From these measurements, they deduced that upon increasing T, there is a rapid increase of ungapped regions. However, even above T_c there still remain some gapped regions. Furthermore, Yazdani *et al.* extracted a relation between a given gap Δ below T_c and the temperature T_p at which it collapses. They did this by first computing the percentage of the sample that is still gapped at a certain T and then compute the probability $P(< \Delta)$ that the size of a gap is less than a given local Δ. Then they stated that a linear relationship between Δ and T_p requires that the x-axes of these two computations are related by a simple ratio. Indeed, they found the ratio $2\Delta/k_B T_p = 7.8 \pm 0.3$.

Subsequently, the article treats optimally doped samples. Experiments were done on the sample OP93 (where OP stands for optimally doped). For this sample, at $T < T_c$, the experiments point out that there indeed is a d-wave pairing gap (similar to the overdoped samples). However, the sample is still entirely gapped 10 K above T_c (unlike the overdoped samples), thus the loss of phase coherence when increasing the temperature above T_c does not affect the presence of the gap; the distribution of gaps just above and below T_c is very similar. When the temperature is increased further, there finally is an inhomogeneous collapse of gaps similar to the collapse in overdoped samples.
The $T_p - \Delta$ ratio found in overdoped samples is then tested for various dopings. It turns out that all measured overdoped and optimally doped samples satisfy this ratio. Note that the ratio looks like the ratio found in BCS theory (see 2.2), namely $2\Delta/k_BT_c = 3.52$. This is an argument to interpret the gaps in the pseudogap phase as indeed being due to pairing. However, the rate is larger than the rate for BCS, thus indicating that the gap is more robust.

Finally, underdoped samples were examined. Unfortunately, it turns out that these samples do not satisfy the same ratio as overdoped and optimally doped samples. The reason is probably that there are now two energy scales that should be taken into account, of which there is only one related to pairing. Namely, over 30% of the measured spectra for $T \ll T_c$ show strange 'kinks', from which we should probably conclude that there is a lower energy scale that is important. Further research is necessary to find out how things work exactly in the underdoped regime.

To summarize, Yazdani *et al.* concluded that phase coherence and formation of Cooper pairs do not occur at the same time, in contrast to conventional superconductors. Instead, first the Cooper pairs are formed (below a temperature T_p), which results in the development of small islands of gapped regions (i.e. the pseudogap phase). Upon lowering the temperature below T_c, the gapped islands merge, phase coherence takes place and the material becomes superconducting. For overdoped and optimally doped samples, the local pairing criterion $2\Delta/k_BT_p = 7.9 \pm 0.5$ is found. This criterion indicates that the gap is more robust than the one in BCS theory. Pairing occurs at T_p and the T^* line (see Fig. 3.2) is controlled by the largest pairing gaps ($T_{p,max}$). In underdoped samples, there are two energy scales. Consequently, these samples do not satisfy the local pairing criterion. The T^* line is controlled by the largest of the two energy scales and seems to be unrelated to pairing. Thus, the $T_{p,max}$ line probably lies well below T^* in the underdoped region. It remains unknown what exactly happens in this region.

Conclusions and outlook

In this thesis, I have made an attempt to give an overview of superconductors in general. Hereby, I have started with low-temperature superconductors, which we saw are well-explained by BCS theory. Subsequently, I have treated high-temperature superconductors and especially cuprates, for which it became clear that ordinary BCS theory does not give an appropriate description. There is no theory that fully describes the high-temperature superconductors and explains how they work.
Our dream is to find materials that become superconducting around room-temperature. However, the realization of this dream still seems to be far away. To make progress we first need to understand the mechanism behind high-T_c superconductivity. To do this, it is especially important to improve the experimental techniques such as ARPES, STM and neutron scattering and to keep searching for new classes of materials that might turn out to be high-T_c superconductors.

The three most studied types of high-T_c superconductors are LSCO, YBCO and BiSCCO. The biggest problem is that the different experimental techniques used on these superconductors all yield results on different time scales, which makes them very difficult to be compared. Because of this, there are many properties of which we do not know if they are universal or specific of a certain material. For example, for LSCO, it is easy to make large samples, which are good for neutron scattering measurements (which yields information in k-space), but its surface is not very flat and the material is dirty, which makes it difficult to do STM and ARPES measurements (which yield information in real space). For BiSCCO, it is exactly the opposite. The surface is very flat, which makes it easy to do STM and ARPES measurements. However, the samples are very small which makes neutron scattering impossible. Then we also have YBCO, where there is an additional complication, namely the presence of Cu-O chains in the material. Because of this, these three high-T_c superconductors are difficult to compare.

As mentioned before, there is no satisfactory theory that explains all properties of the cuprates. Nevertheless, a great step forward seems to have been made by the Yazdani group [10] when they found a relation between the superconducting energy gap and the temperature T_p at which the gap is no longer measurable. This is called the local pairing criterion and it has the form $2\Delta/k_BT_p = 7.9 \pm 0.5$. This criterion is very similar to the criterion found in BCS theory, namely $2\Delta/k_BT_c = 3.52$. Maybe this discovery could lead to a theory for high-T_c superconductors which is an adjusted form of BCS theory. Such a theory would have to explain the robustness of this local pairing criterion (i.e. the factor 7.9 which is much larger than 3.5) and also the other properties of high-T_c superconductors, for example the shape of the phase diagram and the mechanism that lies beneath the formation of gapped islands in the pseudogap phase.

I conclude this thesis by saying that I think there certainly is hope that somewhere in the future, we will be able to give an appropriate description of high-temperature superconductivity. Furthermore, I think that when we have done so, we will be able to say whether or not it is possible to create room-temperature superconductors. Nevertheless, a long road probably lies ahead of us.

Appendix A

Derivation of second quantized operators

To derive the general form of observables in second quantization, we first derive two special cases, namely the kinetic energy T and the two-body interaction V. This derivation is based on ref. [3].
We start with the kinetic energy, $T = \sum_{i=1}^{N} \frac{p_i^2}{2m}$. Now we want to derive the form of this operator in terms of $a_{\mathbf{k}\sigma}$ and $a_{\mathbf{k}\sigma}^\dagger$. We expect

$$T = \sum_{\mathbf{k},\sigma} \frac{|\mathbf{k}|^2}{2m} a_{\mathbf{k}\sigma}^\dagger a_{\mathbf{k}\sigma}, \tag{A.1}$$

because $a_{\mathbf{k}\sigma}^\dagger a_{\mathbf{k}\sigma}$ is the number of particles in the state $|\mathbf{k},\sigma\rangle = |k\rangle$. Note that we have set $\hbar = 1$. We know that T acts on an N-particle state as

$$T|k_1,\ldots,k_N\rangle_\pm = \left(\sum_{i=1}^{N} \frac{|\mathbf{k}_i|^2}{2m}\right)|k_1,\ldots,k_N\rangle_\pm = \left(\sum_{i=1}^{N} \frac{|\mathbf{k}_i|^2}{2m}\right) a_{k_1}^\dagger \cdots a_{k_N}^\dagger |0\rangle,$$

where the $\pm$-sign denotes the symmetry of the state, $+$ or symmetric for bosons and $-$ or antisymmetric for fermions. To prove that equation (A.1) is correct we need to prove that it acts in the same way as above. Using the commutation relations, we obtain

$$\begin{aligned}
(a_k^\dagger a_k) a_{k_1}^\dagger \cdots a_{k_N}^\dagger |0\rangle &= a_k^\dagger(\delta_{kk_1} + \varepsilon a_{k_1}^\dagger a_k) a_{k_2}^\dagger \ldots a_{k_N}^\dagger |0\rangle \\
&= \delta_{kk_1} a_k^\dagger a_{k_2}^\dagger \cdots a_{k_N}^\dagger |0\rangle + \varepsilon a_k^\dagger a_{k_1}^\dagger a_k a_{k_2}^\dagger a_{k_3}^\dagger \cdots a_{k_N}^\dagger |0\rangle \\
&= \delta_{kk_1} a_k^\dagger a_{k_2}^\dagger \cdots a_{k_N}^\dagger |0\rangle + \varepsilon \delta_{kk_2} a_k^\dagger a_{k_1}^\dagger a_{k_3}^\dagger \cdots a_{k_N}^\dagger |0\rangle + \varepsilon^2 a_k^\dagger a_{k_1}^\dagger a_{k_2}^\dagger a_k a_{k_3}^\dagger \cdots a_{k_N}^\dagger |0\rangle \\
&= \\
&\vdots \\
&= \left(\sum_{i=1}^{N} \delta_{kk_i} \varepsilon^{i-1}\right) a_{k_1}^\dagger \cdots a_{k_N}^\dagger |0\rangle,
\end{aligned}$$

where we repeated this process until we can use $a_k|0\rangle = 0$ and $\varepsilon = \pm 1$, $+$ for bosons and $-$ for fermions. After the third equality we used $\varepsilon a_k^\dagger a_{k_1}^\dagger = a_{k_1}^\dagger a_k^\dagger$ in the second term. Then we obtain

$$\begin{aligned}\left(\sum_k \frac{|\mathbf{k}|^2}{2m} a_{\mathbf{k}\sigma}^\dagger a_{\mathbf{k}\sigma}\right) a_{k_1}^\dagger \cdots a_{k_N}^\dagger |0\rangle &= \left(\sum_k \sum_{i=1}^N \frac{|\mathbf{k}|^2}{2m} \delta_{\mathbf{k}\mathbf{k}_i}\right) a_{k_1}^\dagger \cdots a_{k_N}^\dagger |0\rangle \\ &= \left(\sum_{i=1}^N \frac{|\mathbf{k}_i|^2}{2m}\right) a_{k_1}^\dagger \cdots a_{k_N}^\dagger |0\rangle,\end{aligned}$$

which completes the proof. Now, we rewrite T in the $|x\rangle = |\mathbf{r},\sigma\rangle$-basis, using

$$\begin{aligned}a_{\mathbf{k}\sigma}^\dagger &= \frac{1}{V^{\frac{1}{2}}} \int_V d\mathbf{r}\; e^{i\mathbf{k}\cdot\mathbf{r}} \psi_\sigma^\dagger(\mathbf{r}) \\ a_{\mathbf{k}\sigma} &= \frac{1}{V^{\frac{1}{2}}} \int_V d\mathbf{r}\; e^{-i\mathbf{k}\cdot\mathbf{r}} \psi_\sigma(\mathbf{r}),\end{aligned}$$

such that

$$\begin{aligned}T &= \sum_\sigma \frac{1}{V} \int_V d\mathbf{r} \int_V d\mathbf{r}' \left(\sum_{\mathbf{k}} e^{i\mathbf{k}\cdot(\mathbf{r}-\mathbf{r}')} \frac{|\mathbf{k}|^2}{2m}\right) \psi_\sigma^\dagger(\mathbf{r}) \psi_\sigma(\mathbf{r}') \\ &= \sum_\sigma \int_V d\mathbf{r} \int_V d\mathbf{r}'\; \psi_\sigma^\dagger(\mathbf{r}) \delta(\mathbf{r}-\mathbf{r}') \left(-\frac{\hbar^2}{2m}\Delta_{\mathbf{r}'}\right) \psi_\sigma(\mathbf{r}'),\end{aligned}$$

where we used

$$\frac{1}{V}\sum_{\mathbf{k}} e^{i\mathbf{k}\cdot(\mathbf{r}-\mathbf{r}')} \frac{|\mathbf{k}|^2}{2m} = \left\langle \mathbf{r} \left| \frac{p^2}{2m} \right| \mathbf{r}' \right\rangle = \delta(\mathbf{r}-\mathbf{r}') \left(-\frac{\hbar^2}{2m}\Delta_{\mathbf{r}'}\right).$$

Thus, we now have an expression for the kinetic energy in second quantization in the $|\mathbf{r},\sigma\rangle$-basis. From this, the general form of one-body observables A in second quantization can be deduced. Namely,

$$A = \sum_{i,j} \langle \phi_i | A | \phi_j \rangle a_i^\dagger a_j = \sum_i \alpha_i a_i^\dagger a_i, \tag{A.2}$$

where the second equality only holds if A is diagonal (with $A|\phi_i\rangle = \alpha_i|\phi_i\rangle$).
Now we turn to the two-body interaction. Assume that it is spin independent. It acts as follows:

$$V_2 |x_1,\ldots,x_N\rangle_\pm = \frac{1}{2}\sum_{i\neq j} V_2(\mathbf{r}_i,\mathbf{r}_j)|x_1,\ldots,x_N\rangle_\pm \tag{A.3}$$

We claim that the second quantized expression is

$$V_2 = \frac{1}{2}\int dx \int dx'\; V_2(x,x')\psi^\dagger(x)\psi^\dagger(x')\psi(x')\psi(x), \tag{A.4}$$

thus we have to prove that this expression acts on a state in the same way as equation (A.3). The idea is again to bring $\psi(x')\psi(x)$ on $|0\rangle$ using the commutation relations and then use that $\psi(x')\psi(x)|0\rangle = 0$. For simplicity, we first consider $N = 2$. Then we have

$$\begin{aligned}\psi(x)\psi^\dagger(x_1)\psi^\dagger(x_2) &= \delta(x-x_1)\psi^\dagger(x_2) + \varepsilon\psi^\dagger(x_1)\psi(x)\psi^\dagger(x_2) \\ &= \delta(x-x_1)\psi^\dagger(x_2) + \varepsilon\delta(x-x_2)\psi^\dagger(x_1) + \varepsilon^2\psi^\dagger(x_1)\psi^\dagger(x_2)\psi(x),\end{aligned}$$

and therefore

$$\begin{aligned}\psi(x')\psi(x)\psi^\dagger(x_1)\psi^\dagger(x_2) &= \delta(x-x_1)\psi(x')\psi^\dagger(x_2)+\varepsilon\delta(x-x_2)\psi(x')\psi^\dagger(x_1)+\varepsilon^2\psi(x')\psi^\dagger(x_1)\psi^\dagger(x_2)\psi(x)\\ &= \delta(x-x_1)\delta(x'-x_2)+\varepsilon\delta(x-x_1)\psi^\dagger(x_2)\psi(x')+\varepsilon\delta(x-x_2)\delta(x'-x_1)\\ &\quad+\varepsilon^2\delta(x-x_2)\psi^\dagger(x_1)\psi(x')+\varepsilon^2\delta(x'-x_1)\psi^\dagger(x_2)\psi(x)+\varepsilon^3\psi^\dagger(x_1)\psi(x')\psi^\dagger(x_2)\psi(x)\\ &= \delta(x-x_1)\delta(x'-x_2)+\varepsilon\delta(x-x_1)\psi^\dagger(x_2)\psi(x')+\varepsilon\delta(x-x_2)\delta(x'-x_1)\\ &\quad+\varepsilon^2\big[\delta(x-x_2)\psi^\dagger(x_1)\psi(x')+\delta(x'-x_1)\psi^\dagger(x_2)\psi(x)+\varepsilon\delta(x'-x_2)\psi^\dagger(x_1)\psi(x)\\ &\quad+\varepsilon^2\psi^\dagger(x_1)\psi^\dagger(x_2)\psi(x')\psi(x)\big].\end{aligned}$$

Applying this state on the vacuum $|0\rangle$ gives

$$\psi(x')\psi(x)\psi^\dagger(x_1)\psi^\dagger(x_2)|0\rangle = \big(\delta(x-x_1)\delta(x'-x_2)+\varepsilon\delta(x-x_2)\delta(x'-x_1)\big)\,|0\rangle.$$

Then, recalling that $\varepsilon^2=1$, we obtain

$$\begin{aligned}\psi^\dagger(x)\psi^\dagger(x')\psi(x')\psi(x)\psi^\dagger(x_1)\psi^\dagger(x_2) &= \delta(x-x_1)\delta(x'-x_2)\psi^\dagger(x)\psi^\dagger(x')|0\rangle\\ &\quad+\varepsilon\delta(x-x_2)\delta(x'-x_1)\psi^\dagger(x)\psi^\dagger(x')|0\rangle\\ &= \delta(x-x_1)\delta(x'-x_2)\psi^\dagger(x_1)\psi^\dagger(x_2)|0\rangle\\ &\quad+\varepsilon\delta(x-x_2)\delta(x'-x_1)\psi^\dagger(x_2)\psi^\dagger(x_1)|0\rangle\\ &= \big[\delta(x-x_1)\delta(x'-x_2)+\delta(x-x_2)\delta(x'-x_1)\big]\,\psi^\dagger(x_1)\psi^\dagger(x_2)|0\rangle,\end{aligned}$$

where in the last step we exchanged particles in the second term, which yielded another ε. Now we multiply by $V_2(x,x')$ and integrate over x and x'. This yields

$$\begin{aligned}&\int dx\int dx'\,\big(\delta(x-x_1)\delta(x'-x_2)+\delta(x-x_2)\delta(x'-x_1)\big)\,V_2(x,x')\psi^\dagger(x_1)\psi^\dagger(x_2)|0\rangle\\ &= V_2(x_1,x_2)\psi^\dagger(x_1)\psi^\dagger(x_2)|0\rangle+V_2(x_2,x_1)\psi^\dagger(x_1)\psi^\dagger(x_2)|0\rangle\\ &= 2V_2(x_1,x_2)|x_1,x_2\rangle_\pm,\end{aligned}$$

where in the last step we used that the potential is symmetric in x_1 and x_2. This proves equation (A.4) for two particles. The N-particle case can be done in a similar way.
We go to momentum space by plugging in the Fourier transforms given by

$$\psi^\dagger(\mathbf{r}) = \frac{1}{V^{\frac{1}{2}}}\sum_{\mathbf{k}} e^{-i\mathbf{kr}}a^\dagger_{\mathbf{k}\sigma},$$

$$\psi(\mathbf{r}) = \frac{1}{V^{\frac{1}{2}}}\sum_{\mathbf{k}} e^{i\mathbf{kr}}a_{\mathbf{k}\sigma}.$$

This yields

$$V_2 = \frac{1}{2}\sum_{\substack{\mathbf{k_1},\mathbf{k_2},\mathbf{k_3},\mathbf{k_4}\\ \sigma_1,\sigma_2,\sigma_3,\sigma_4}} a^\dagger_{\mathbf{k_1}\sigma_1}a^\dagger_{\mathbf{k_2}\sigma_2}a_{\mathbf{k_3}\sigma_3}a_{\mathbf{k_4}\sigma_4}\langle\mathbf{k_1},\sigma_1;\mathbf{k_2},\sigma_2|V_2|\mathbf{k_4},\sigma_4;\mathbf{k_3},\sigma_3\rangle,$$

where

$$\begin{aligned}\langle \mathbf{k_1},\sigma_1;\mathbf{k_2},\sigma_2|V_2|\mathbf{k_4},\sigma_4;\mathbf{k_3},\sigma_3\rangle &= \frac{1}{L^6}\sum_{\sigma,\sigma'}\int_V d\mathbf{r}\int_V d\mathbf{r}'\; e^{-i\mathbf{k_1}\cdot\mathbf{r}}\delta_{\sigma_1\sigma}e^{-i\mathbf{k_2}\cdot\mathbf{r}'}\delta_{\sigma_2\sigma'} \\ &\qquad V_2(\mathbf{r},\sigma;\mathbf{r}',\sigma')e^{i\mathbf{k_4}\cdot\mathbf{r}}\delta_{\sigma_4\sigma}e^{i\mathbf{k_3}\cdot\mathbf{r}}\delta_{\sigma_3\sigma'} \\ &= \frac{1}{L^6}\sum_{\sigma,\sigma'}\delta_{\sigma_1\sigma}\delta_{\sigma_2\sigma'}\delta_{\sigma_4\sigma}\delta_{\sigma_3\sigma'}\int_V d\mathbf{r}\int_V d\mathbf{r}'\; V_2(\mathbf{r}-\mathbf{r}')e^{i(\mathbf{k_4}-\mathbf{k_1})\cdot\mathbf{r}}e^{i(\mathbf{k_3}-\mathbf{k_2})\cdot\mathbf{r}'} \\ &= \frac{1}{L^6}\delta_{\sigma_1\sigma_4}\delta_{\sigma_2\sigma_3}\int_V d\mathbf{r}'\; e^{i(\mathbf{k_3}-\mathbf{k_2})\cdot\mathbf{r}'}\int_V d\tilde{\mathbf{r}}\; e^{i(\mathbf{k_4}-\mathbf{k_1})\cdot(\mathbf{r}'+\tilde{\mathbf{r}})}V_2(\tilde{\mathbf{r}}) \\ &= \frac{1}{L^6}\delta_{\sigma_1\sigma_4}\delta_{\sigma_2\sigma_3}\int_V d\mathbf{r}'\; e^{i(\mathbf{k_3}+\mathbf{k_4}-\mathbf{k_1}-\mathbf{k_2})\cdot\mathbf{r}'}\int_V d\tilde{\mathbf{r}}\; V_2(\tilde{\mathbf{r}})e^{i(\mathbf{k_4}-\mathbf{k_1})\cdot\tilde{\mathbf{r}}} \\ &= \frac{1}{L^3}\delta_{\sigma_1\sigma_4}\delta_{\sigma_2\sigma_3}\delta_{\mathbf{k_3}+\mathbf{k_4},\mathbf{k_1}+\mathbf{k_2}}\widetilde{V}_2(\mathbf{k_1}-\mathbf{k_4}),\end{aligned}$$

assuming that $V_2(x,x') = V_2(\mathbf{r}-\mathbf{r}')$ such that we could explicitly do the summation over σ,σ'. Then

$$\begin{aligned}V_2 &= \frac{1}{2L^3}\sum_{\substack{\mathbf{k_1},\mathbf{k_2},\mathbf{k_3},\mathbf{k_4}\\ \sigma_1,\sigma_2,\sigma_3,\sigma_4}} a^\dagger_{\mathbf{k_1}\sigma_1}a^\dagger_{\mathbf{k_2}\sigma_2}a_{\mathbf{k_3}\sigma_3}a_{\mathbf{k_4}\sigma_4}\delta_{\sigma_1\sigma_4}\delta_{\sigma_2\sigma_3}\delta_{\mathbf{k_3}+\mathbf{k_4},\mathbf{k_1}+\mathbf{k_2}}\widetilde{V}_2(\mathbf{k_1}-\mathbf{k_4}) \\ &= \frac{1}{2L^3}\sum_{\substack{\mathbf{k_1},\mathbf{k_2},\mathbf{k_3},\mathbf{k_4}\\ \sigma,\sigma'}} a^\dagger_{\mathbf{k_1}\sigma}a^\dagger_{\mathbf{k_2}\sigma'}a_{\mathbf{k_3}\sigma'}a_{\mathbf{k_4}\sigma}\delta_{\mathbf{k_3}+\mathbf{k_4},\mathbf{k_1}+\mathbf{k_2}}\widetilde{V}_2(\mathbf{k_1}-\mathbf{k_4}) \\ &= \frac{1}{2L^3}\sum_{\substack{\mathbf{k},\mathbf{k}',\mathbf{q}\\ \sigma,\sigma'}}\widetilde{V}_2(\mathbf{q})a^\dagger_{\mathbf{k}+\mathbf{q}\sigma}a^\dagger_{\mathbf{k}'-\mathbf{q}\sigma'}a_{\mathbf{k}'\sigma'}a_{\mathbf{k}\sigma}\end{aligned} \tag{A.5}$$

where we defined $\widetilde{V}_2(\mathbf{q}) := \int_V d\mathbf{r}\; V_2(\mathbf{r})e^{-i\mathbf{q}\cdot\mathbf{r}}$ and set $\sigma_1 = \sigma_4 =: \sigma$ and $\sigma_2 = \sigma_3 =: \sigma'$ and $\mathbf{k_1}-\mathbf{k_4} = \mathbf{q}$, $\mathbf{k_4} = \mathbf{k}$ and $\mathbf{k_3} = \mathbf{k}'$ by using the Kronecker delta's.
From this we can deduce the general form for two-body observables in second quantization, namely

$$V_2 = \frac{1}{2}\sum_{i,j,k,l} V_{ij;kl}a^\dagger_i a^\dagger_j a_l a_k,$$

where $V_{ij;kl} = \langle\phi_i\otimes\phi_j|V|\phi_k\otimes\phi_l\rangle$.

Appendix B

Scanning Tunneling Microscopy (STM)

STS, or Scanning Tunneling Spectroscopy, is an experimental technique with which we can obtain information about the atomic and electronic structure of materials. STM, which is a specific branch of STS, is for instance used for measurements on the high-T_c superconductor BiSCCO. In this appendix, I will briefly discuss this technique. Hereby I have mainly used ref. [11].

Consider two electrodes, separated by an insulating barrier. Then, if the wave functions of the electrons overlap, they can tunnel through this barrier. The number of electrons that will go through is dependent on the electronic structure of the electrodes and the distance between them. If you measure the tunneling current, it is thus possible to obtain information on the electronic structure and topography of the electrodes. This is the principle on which STS is based.
In 1961, Ivar Giaever was the first one to apply quasi-particle tunneling as a method of scanning. As electrodes, he used an aluminium and a lead sheet and as insulating barrier, he used an aluminium-oxide plane with width $\sim \mathring{A}$. He varied the bias-voltage over the two sheets. Subsequently, he could measure the differential tunneling conductance dI/dV. Furthermore, he could control whether lead was in the normal or superconducting state upon applying a magnetic field. With these experiments, Giaever confirmed the BCS theory.
However, with this method of scanning, it is not possible to indicate from which site of the sample or probe the tunneling electron that produced the current originated. In 1981, Rohrer and Binnig invented the Scanning Tunneling Microscope with which this was possible. This discovery was a great revolution because it was the first time that we could actually see individual atoms. The microscope uses an electrode with atomic width (like a very thin needle) instead of a sheet electrode. This probe comes so close to the sample that the wave functions overlap, such that, when a voltage difference is applied between the probe and the sample, electrons can tunnel through the space between the sample and the probe. Consequently, a current starts flowing. This current is strongly dependent on the precise distance between the probe and the sample, thus it can be changed by moving the probe. With this method it was possible for the first time to acquire electronic and atomic information of specific sites of the sample. The microscope can measure displacements $\sim 10^{-12}\ m$ and energy differences $\sim 600\ \mu V$, thus it is very precise. However, there is also a downside. Namely, the preciseness makes the microscope also very sensitive to external influences, which complicates the measurements. To make the measurements as precise as possible, the space between the probe

and the sample should be a perfect vacuum, but this is difficult to realize.
To make a three-dimensional image of a sample, there are two methods that can be used. For both of these methods we need the electrons to be homogeneously arranged through the sample, i.e. the local (electron) density of states (LDOS) must be homogeneous. The first method, Constant Current Imaging, consists of letting the probe move over the sample in such a way that the tunneling current is always constant. For the second method, Constant Height Imaging, the height is kept constant. This method is remarkably easier and faster, but there is a risk that the probe breaks because it hits an irregularity in the sample.
It turns out that there is a direct relation between dI/dV and the spectral function and therefore the local density of states. Then dI/dV can be measured by changing the bias voltage while holding the probe at a fixed position.

In order to do STM measurements on BiSCCO, the used samples cannot contain too many irregularities (because then the probe will probably break). It is possible to make samples that are flat enough by cutting the crystal precisely between two BiO planes. We can do this because the bonds between two BiO planes are weaker than the other bonds in the BiSCCO crystal. Furthermore, because the movement of the electrons is restricted to the CuO_2 planes (see 3.3.2), we neglect the BiO and SrO planes completely and suppose that what we are probing when looking at the BiO plane are actually the electrons in the CuO_2 plane beneath. But we cannot be sure that this is indeed the case.

Bibliography

[1] D.B.M. Dickerscheid, K.B. Gubbels, and H.T.C. Stoof. *Ultracold Quantum Fields*, pages 109–128. Springer, 2009.

[2] H. Bruus and K. Flensberg. *Many-body Quantum Theory in Condensed Matter Physics - an introduction*, pages 1–31. Oxford University Press, 2nd edition, 2002.

[3] C. de Morais Smith. *Chapter 2: Second quantization, electrons and phonons*. Lecture notes, 2006.

[4] C. de Morais Smith. Hand-written lecture notes, 2006.

[5] C. de Morais Smith. *Superconductivity*. Lecture notes, 2006.

[6] C. de Morais Smith. *Microscopic theory: BCS theory (Bardeen, Cooper and Schrieffer theory)*. Lecture notes, 2006.

[7] J.C. Everts. *Topological phases and fermionic superfluidity on the Lieb lattice*. Master's thesis, Utrecht University, 2012.

[8] Chandra Varma. *Mind the pseudogap*. ***Nature***, 468:184–185, 2010.

[9] G. S. Boebinger, Y. Ando, A. Passner, T. Kimura, M. Okuya, J. Shimoyama, K. Kishio, K. Tamasaku, N. Ichikawa, and S. Uchida. *Insulator-to-Metal Crossover in the Normal State of La2-xSrxCuO4 Near Optimum Doping*. ***Phys. Rev. Lett.***, 77:5417–5420, 1996.

[10] K.K. Gomes, A.N. Pasupathy, A. Pushp, S. Ono, Y. Ando, and A. Yazdani. *Visualizing pair formation on the atomic scale in the high-T_c superconductor $Bi_2Sr_2CaCu_2O_{8+\delta}$*. ***Nature***, 447:569–572, 2007.

[11] N. de Jeu. *Theoretical studies of Scanning Tunneling Microscopy of high-T_c superconductors*. Master's thesis, Utrecht University, 2007.